Therapeutic potential of astrocytes via *in vivo* expression of reprogramming factor in mouse models of cerebral ischemia

Jung Hwa Seo

Department of Medical Science

The Graduate School, Yonsei University

Therapeutic potential of astrocytes via *in vivo* expression of reprogramming factor in mouse models of cerebral ischemia

Jung Hwa Seo

Department of Medical Science

The Graduate School, Yonsei University

Therapeutic potential of astrocytes via *in vivo* expression of reprogramming factor in mouse models of cerebral ischemia

Directed by Professor Sung-Rae Cho

The Doctoral Dissertation
submitted to the Department of Medical Science
the Graduate School of Yonsei University
in partial fulfillment of the requirements for the degree of
Doctor of Philosophy of Medical Science

Jung Hwa Seo

June 2018

This certifies that the Doctoral Dissertation of
Jung Hwa Seo is approved.

Thesis Supervisor: Sung-Rae Cho

Thesis Committee Member #1: Hyongbum Kim

Thesis Committee Member #2: Jong Eun Lee

Thesis Committee Member #3: Se Hoon Kim

Thesis Committee Member #4: Sung Hoon Kim

The Graduate School
Yonsei University

June 2018

ACKNOWLEDGEMENTS

2009년 처음 이곳에 발을 디딘 후 현재까지 이끌어 주신 조성래 교수님, 교수님 덕분에 재활의학이라는 분야에 한 걸음 다가갈 수 있었고, 깊이 있는 동물 실험도 배울 수 있었습니다. 연구는 새로운 발견이라고 하셨던 교수님 말씀 깊이 새기고 연구에 대한 호기심을 잃지 않겠습니다. 석사 때부터 도움주신 김형범 교수님, 한 분야의 전문가로서 도전적인 모습이 인상적 이였습니다. 함께 공동 연구를 진행하면서 연구의 방향설정과 실험계획을 어떻게 해야 하는지에 대한 것들을 배울 수 있어서 영광이었습니다. 이종은 교수님께서 말씀해 주신 박사학위를 받는 학생의 자세와 연구에 대한 신념이 중요하다는 것을 느꼈고 부족한 저에게 소중한 가르침 주신 것에 감사드립니다. 김세훈 교수님께서는 제가 미처 생각하지 못하고 오류가 있었던 것들에 대해 설명해 주시고 조언해 주셔서 많은 도움이 되었고 앞으로의 연구에 중요한 기초가 될 것 같습니다. 마지막으로 김성훈 교수님, 연구의 깊이가 깊어질 수 있게 조언 주신 부분들을 잊지 않겠습니다.

바쁘신 중에 자문 및 심사를 위해 귀중한 시간 내어 주신 모든 교수님들께 다시 한 번 감사의 인사 올립니다.

이곳에서 여러 해를 보내는 동안 도움 주신 많은 분들이 있었습니다. 먼저 우리 재활의학교실 식구들, 여러분 덕분에 실험실 생활이 즐거웠습니다. 이곳 생활의 처음과 끝을 함께한 유지혜 박사님, 처음 우리가 만났을 때 박사학위라는 커다란 산을 함께 넘게 될 줄은 몰랐는데 우여곡절 끝에 여기까지 함께 올 수 있어서 천만다행입니다. 앞으로도 서로에게 힘이 되어주는 친구로 남고 싶습니다. 박사과정을 함께한 위수현 선생님, 힘들 때 긍정적인 말들로 위로해 주고 연구의 마무리 과정을 함께해 주어서 큰 힘이 되었습니다. 학위과정을 함께해준 김민지 선생님도 어려움이 있을 때 자기일처럼 도움을 주어서 고맙습니다. 박사학위를 함께 시작했던 신윤겸 선생님, 비록 내가 먼저 졸업하지만 항상 열심히 연구하는 선생님이 졸업할 때는 더 의미 있는 연구결과로 졸업하리란 것을 의심치 않습니다. 항상 바쁘게 움직이는 백아름 박사님, 열심히 하는 모습이 보기 좋고 함께 연구하는 동안 도움을

많이 받아서 감사하게 생각하고 있습니다. 박사과정중인 송석영, 조은주 선생님 그리고 실험실 막내 남배근, 표순일. 아직 갈길이 멀었지만 지금처럼 열심히 해서 좋은 결과 있길 바랍니다.

나의 연구과정에서의 롤모델인 신소라 박사님, 어려운 상황에 부딪혀도 결국엔 이겨내는 박사님 모습은 멘탈이 강하지 못한 저에겐 충격이었습니다. 너무도 닮고 싶은 박사님을 보며 여기까지 왔지만 아직도 부족함이 많습니다. 앞으로도 많은 조언 부탁합니다. 소아과의 김미리 선생님, 신경과의 조인자 선생님, 비록 다른 실험실에 있지만 같은 실험실 동료처럼 챙겨주고 다독여 주어서 가끔 있는 행운처럼 반가웠습니다. 새로운 실험과 기초지식을 성심껏 알려주신 약리학교실 신정홍 선생님께도 이 자리를 빌어 고마운 마음 전합니다.

사랑하는 가족들, 부모님과 언니, 그리고 동생. 언제나 곁에서 힘이 되어주고 응원해 주어서 고맙습니다. 단짝친구 김가미에게도 지금까지 함께해 주어서 고맙고 앞으로도 서로 의지할 수 있는 영원한 친구로 남고 싶단말 전하고 싶습니다. 마지막으로 졸업할 때까지 지원을 아끼지 않았던 남편 김용국, 고맙고 사랑합니다.

처음 신경과학에 대한 막연한 호기심으로 시작한 연구원 생활이 뇌성마비에서의 줄기세포 치료, 뇌졸중에서의 생체내 리프로그래밍을 거쳐 신경퇴행성 질환에서의 유전자 교정 치료까지 연구하며 박사학위를 마치게 될 줄은 상상도 못했습니다. 이곳에 오기까지 여러분들의 도움이 없었다면 포기했을 지도 모릅니다.
앞으로 10년, 20년 뒤의 내가 어떤 모습일지 모르겠지만, 지금까지의 경험들이 그때의 저를 만들고 있겠지요. 항상 감사하는 마음으로 발전하는 사람이 되겠습니다. 감사합니다.

2018년 6월
서 정 화

TABLE OF CONTENS

LIST OF FIGURES

LIST OF TABLES

ABSTRACT

Therapeutic potential of astrocytes via *in vivo* expression of reprogramming factor in mouse models of cerebral ischemia

Jung Hwa Seo

Department of Medical Science

The Graduate School, Yonsei University

(Directed by Professor Sung-Rae Cho)

Cerebral ischemia and stroke can lead incurable brain damage or death. Astrocytes, one of the most abundant cells in the brain, are activated by injury such as ischemia. Reactive astrocytes, in particular, play a crucial role in recovery from brain injury. Four reprogramming factors (Pou5f1, Sox2, Myc, and Klf4) expression have been used to convert cell types, but it has rarely been studied promoting functional recovery by expression of reprogramming factors in ischemic injury. The aim of this study is therefore to determine whether *in vivo* transient expression of reprogramming factor can improve neurobehavioral function.

Cerebral ischemia was induced by two methods—transient bilateral common carotid artery occlusion (BCCAO) and permanent unilateral common carotid artery ligation with hypoxia (8% O_2)—after which brains were treated (in the lateral ventricle or striatum) with doxycycline (DOX) in transgenic mice in which

the four reprogramming factors were expressed by doxycycline. Either doxycycline (DOX-1; 1 μg/ml, DOX-100; 100 μg/ml) or phosphate-buffered saline (PBS) was then infused into the brain via an osmotic pump for 7 days.

In the BCCAO model, histologic evaluation showed that this transient expression of reprogramming factor induced the proliferation of astrocytes and neural progenitors, while neurons and glial scar formation was not observed. Furthermore, *in vivo* expression of reprogramming factor caused neuroprotective effects and angiogenesis in the striatum. Tumor formation was not observed in any group. Importantly, the rotarod and ladder walking tests showed to promote functional restoration from ischemic damage via the expression of the four reprogramming factors. To elucidate the therapeutic mechanisms associated with astrogliosis, RNA sequencing analysis was performed in order to identify a transcriptome that was significantly changed in the DOX-100 group compared to PBS group. Among downregulated genes (complement C3, C4a, C4b, C1qa, C1qb and C1qc) and astrocyte markers (GFAP, Vimentin and S100β) were validated using qRT-PCR. Because C3 is a detrimental astrocyte marker, C3 in particular was measured using histologic analysis. The results showed that C3 was significantly reduced in DOX-100 treated mice compared with the DOX-1 and PBS groups.

A hypoxic-ischemic (HI) model, a stroke model used in another experimental group, was used to compare efficacy of reprogrammed expression in two areas of the brain, the ventricle and striatum. That results showed that the astrocytes and neural progenitors were significantly proliferated, but not neurons or glial scar, and the condition of blood vessels in the injured brain was improved following *in vivo* reprogramming factor expression. Furthermore, *in vivo* reprogramming factor expression was protective of neurons under hypoxic ischemic conditions. Notably, neurobehavioral evaluations such as the grip strength, cylinder, ladder walking and open field tests showed functional recovery was dramatically improved via the expression of the four reprogramming factors in the lateral

ventricle. Interestingly, the expression of the reprogramming factors in the striatum did not lead to changes in neurological function in any group. In the rotarod test, there were no significant differences in both the lateral ventricular-targeted and striatum-targeted group. Tumor development was not observed in the lateral ventricle-targeted group, but the striatum-targeted group showed that abnormal cell proliferation in DOX-100 treated mice brain. Furthermore, treatment with DOX-1,000 (doxycycline; 1,000 μg/ml) lead to tumor formation in the striatum-targeted group.

Taken together, newly generated astrocytes are essential for protecting neurons from damage following cerebral ischemia (BCCAO and HI mouse model) and for enhancing blood vessels. These results show that a therapeutic potential of methods that aim to improve functional recovery by reducing reactive astrocytes (harmful A1 astrocytes) in BCCAO mouse models. In the HI mouse model, we noted a recovery effect in the group in which the lateral ventricle was targeted with the expression of reprogramming factors, but not in the striatum-targeted group. Therefore, targeting the lateral ventricle for expression of reprogramming factors may offer better therapeutic results.

Key words: reprogramming factor, cerebral ischemia, functional recovery, reactive astrocyte, neuroprotection

Therapeutic potential of astrocytes via *in vivo* expression of reprogramming factor in mouse models of cerebral ischemia

Jung Hwa Seo

Department of Medical Science

The Graduate School, Yonsei University

(Directed by Professor Sung-Rae Cho)

I. INTRODUCTION

1. Cerebral ischemia models

A. Bilateral common carotid artery occlusion (BCCAO) mouse model

Transient global cerebral ischemia has been caused by 2-vessel-occlusion rodent models.[1,2] This 2-vessel-occlusion model is another name for bilateral carotid artery occlusion (BCCAO), which is one of the ischemic stroke models. Transient ischemic insult leads to selective damage in different brain regions according to ischemic time. Hippocampal damage has been induced by an ischemic duration of 3~10 minutes, and after 20~30 minutes under ischemic conditions, damage can be observed in the form of neuronal death in the striatum and cortex in rodent models.[3,4] Transient BCCAO models are able to create mild brain injury via easy surgical methods, there is also an additional advantage in terms of survival rate. Induction of global cerebral ischemia on both sides of brain

has been shown to lead to behavioral motor deficits associated with grip power,[5] so this model is considered to be appropriate for the investigation of motor function.

B. Hypoxic-ischemic (HI) stroke mouse model

Stroke is the most common disease causing long-term damage in lifetime, and hypoxic-ischemic stroke is a well-known stroke model that can be quickly established in rodent models using simple surgical skills.[6,7] Hypoxic environments lead to coagulation on the ipsilateral side of the brain after permanent ligation of the common carotid artery. Hypoxic-ischemic (HI) stroke models create damage in the cortex, hippocampus, and striatum, while the other side was only affected by the hypoxia condition.[6,8] Importantly, HI models create neurological impairments that are similar to those seen in human stroke.[6] Therefore, the hypoxic-ischemic stroke model is a well-established rodent model that may show asymmetrical behaviors.

2. Restorative therapy in brain disease

Restoration or regeneration of damaged tissue is important for recovery of neurobehavioral function from injury or disease.[9] The brain deficits capacity of restoration, including injured brain tissues often leads to semi-permanent functional impairment, in comparison with other organs. Under impaired environment, endogenous cell sources are not sufficient for functional recovery induced via proliferative generation in the brain. therefore, supplementation of other cell types, such as mesenchymal stem cells from adult tissues and neural stem cells, may help recovery.

To overcome this limitation, stem cell grafts have been used experimentally to replace damaged cells. Indeed, intravenous injection of bone marrow mononuclear cells can reduce infarct size and improve functions, and intracerebral transplantation of bone marrow stromal cells lead to differentiate

into penotypic neural cells and recovery motor function in cerebral ischemia rat model.[10,11] Delcroix and colleagues showed that neural stem cells NSCs onto a polymer scaffold can promote brain tissue regeneration in hypoxic ischemic mice.[12] However, the engraftment of cell transplantation is often limited in both survival and differentiation control of grafted cells.[13] And generated neural cells from grafted cells are not sufficient leading to recovery neuronal functions in stroke.[14] Furthermore, there are some concerns in safety and efficacy after cell injections that allogenic or xenogeneic cells can be rejected by the immune system or tumor development.[9,15]

Another form of therapy supplies neurotrophic factors to aid recovery. Previous study has shown that supply of exogenous humoral factors such as epidermal growth factor (EGF) and brain-derived neurotrophic factor (BDNF) enhanced functional recovery via newly generated neurons in neonatal hypoxic ischemic brain injury.[9,16] In Huntington's disease model, adenoviral vector mediated delivery of BDNF and noggin into the lateral ventricle led to striatal regeneration and functional recovery.[17,18] However, stimulation of endogenous cells leading to robust neurobehavioral restoration via these humoral factors are restricted in the cells without receptors for these factors.[9]

3. *In vitro* and *in vivo* reprogramming

Induction of pluripotent stem cells using four reprogamming-associated transcription factors—Pou5f1 (octamer-binding protein, Oct4), Sox2 (SRY-box containing gene 2), Myc (c-myelocytomatosis oncogene, c-myc), and Klf4 (Kruppel-like factor 4)—has been first reported by Yamanaka's group.[19] Since then, many studies have shown direct conversion that transient expression of reprogramming factors to induce specific cell type undergo conversion into other lineages.[9,20-22] Recent study showed that transient acquisition of pluripotent status by reprogramming factors can induce lineage conversion into cardiomyocytes of neural stem cells.[9,23]

Direct lineage conversion using defined reprogramming factors--from fibroblast into neurons and neural progenitors--has been studied for consider practical applications without going through pluripotent status.[9,24,25] Vierbuchen and Wernig demonstrated that disease modeling and therapy of cell replacement could be provided by direct conversion.[9,26] Indeed, *in vitro* CNS disease modeling was reproduced the disease by direct conversion.[9,27,28] This will be an important process for understanding reason of the disease and for seeking therapy. Also, *in vivo* direct reprogramming shown that glial cells and transplanted fibroblasts has been converted into neuronal lineage cells *in vivo*.[29-31] These findings suggest that direct conversion using reprogramming factor can attribute to alterative approach for replacement instead of injured neurons.

4. Regeneration and proliferation via reprogramming factors

One of the earliest noticeable responses of cells that are exposed to forced expression of the four reprogramming factors is enhanced cell proliferation, which can be observed as early as 24 hours after induction of this expression.[9,32] This enhanced proliferative generation is associated with the regulation genes of cell proliferation.[33] In addition, Myc promotes neovascularization[34] that is an essential process for recovery from brain injury induced by ischemia. Lights of this observation, in vivo transient expression of reprogramming factors can be therapeutic potential in ischemic injury trough endogenous cell proliferation and differentiation.

5. Astrocyte response to brain injury

Astrocytes are abundant glial cells found in the central nervous system (CNS), where they serve important functions such as releasing neurotrophic factors for neurons, supporting synaptogenesis, pruning synapses, and maintaining homeostasis.[35-41]

CNS injury, including focal ischemic stroke, neurodegenerative disease, and CNS trauma, induces a heterogenous population of reactive astrocytes (activated astrocytes).[35-37,42,43] The induction of reactive astrocytes is accompanied by changes in cell morphology, proliferation, gene expression, and glial scar formation under pathologic conditions.[36]

Recently, it has been found that reactive astrocytes can be classified into two different types, ‘‘A1s’’ and ‘‘A2s’’, induced by neuroinflammation and ischemia.[44] Studies have suggested that A1s (inflammatory reactive astrocytes) are induced by NFkB signaling,[37,44,45] whereas Anderson et al. have shown that A2s are induced by Stat3, which promotes neuronal regeneration in acute trauma model.[42,44] Moreover, A1s might have harmful functions to destruction of synapse, while A2s have been shown to have beneficial effects, including the upregulation of neurotrophic factors to promote neurogenesis and the survival of neurons.[44]

Therefore, the distinction between different kinds of reactive astrocytes (A1s or A2s) may contribute to the development of therapeutic interventions that promote neurological recovery.

6. Therapeutic target: Reactive astrocytes

The brain tissue consists of neurons and non-neuronal cells such as astrocytes, microglia, oligodendrocytes, and endothelial cells. Microglia are known to regulate innate immunity, and astrocytes possibly play an important role in the immune system in CNS.[35] Because glial cells are sensitive to environmental changes, these the regulation of these cells could play a critical role in restoring function after brain damage.

Astrocytes play many important roles, including the production of trophic factors and metabolites for neurons; the regulation of ion balance, neurotransmitters, and fluid; and the formation of synapses.[46,47] Astrocytes are reactive in many CNS disorders, changing into either neurotoxic A1s or protective A2s.[44]

Zamanian and colleagues have demonstrated that astrocytes respond to brain injuries or diseases, and their phenotype (reactive astrocyte) depends strongly on the type of inducing injury, such as middle cerebral artery occlusion (MCAO) or a systemic injection with lipopolysaccharide (LPS). LPS reactive astrocytes have been shown to express complements such as C1r, C1s, C3, and C4, leading to neuronal and synaptic loss.[48,49] In contrast, reactive astrocytes induced by MCAO have been shown to overexpress neurotrophic factors and cytokines such as LIF, IL-6, thrombospondins, and CLCF1 in order to aid synapse regeneration.[48,50,51] In one study, when C1q-deficient mice received neonatal hypoxic-ischemic brain injury, expression of C3 and cerebral infarct volume significantly decreased in C1q-/- mice compared with wild type mice.[52] The TrkB receptor for BDNF is highly expressed in glial cells in neurological disorders.[46,53] BDNF may also have therapeutic potential, potentially contributing to neuronal survival, axonal growth, and the inhibition of neurotoxicity.[54,55] Moreover, because neurons are not viable without astrocytes, neuroprotective therapeutics should be protective of both neurons and astrocytes.[44,56]

Therefore, a useful therapeutic approach would be to find a way to induce A2-like astrocytes and/or inhibit A1-like astrocytes. These approaches, which protect or proliferate astrocytes, may lead neuroprotection in the ischemic brain.

7. Aims of this study

This study of the therapeutic potential of *in vivo* expression of reprogramming factors in mouse models of cerebral ischemia has three main goals. First, this study aims to determine whether *in vivo* transient expression of reprogramming factors can change endogenous neural cells and enhance functional recovery from ischemic brain injury. To investigate this, cerebral ischemic subjects (BCCAO and HI) were made to perform tests of neurobehavioral function including the rotarod, ladder walking, cylinder, grip strength, and openfield tests, and histological changes were assessed in both the subventricular zone and the striatum. Second, to elucidate the mechanism by which reprogramming factors induce recovery of neurobehavioral function, transcriptome analysis, qRT-PCR for validation, and immunohistochemistry were performed. Finally, to determine the efficient ways of injection for neurorestoration against ischemic brain damage, reprogramming factor was induced in either the lateral ventricle or the striatum.

II. MATERIALS AND METHODS

1. Mice

The reprogrammable mice [Gt(ROSA)26Sor$^{tm1(rtTA*M2)Jae}$ Col1a1$^{tm3(tetO-Pou5f1,-Sox2,-Klf4,-Myc)Jae}$/J], in which the four reprogramming factors Pou5f1, Sox2, Klf4, and Myc are expressed in the presence of doxycycline,[57] were purchased from the Jackson Laboratory (Bar Harbor, ME, USA) (Figure 1). Control C57BL/6J mice were also obtained from the Jackson Laboratory. Mice were housed in a facility accredited by the Association for Assessment and Accreditation of Laboratory Animal Care (AAALAC), were given food and controlled climate conditions with a 12-hour light/dark cycle, and were provided standard food and water ad libitum. Mice of both sexes, aged 8~16 weeks, were used. All procedures were reviewed and approved by the Institutional Animal Care and Use Committee (IACUC) of the Yonsei University College of Medicine (permit number: 2013-0220, 2016-0070).

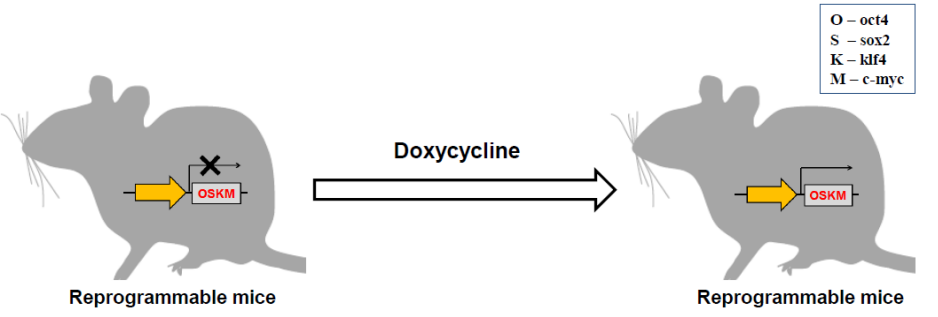

Figure 1. Reprogrammable mice. The reprogrammable mice [Gt(ROSA)26Sor$^{tm1(rtTA*M2)Jae}$ Col1a1$^{tm3(tetO-Pou5f1,-Sox2,-Klf4,-Myc)Jae}$/J] are genetically modified mice, in which the four reprogramming factors Pou5f1, Sox2, Klf4, and Myc are expressed by doxycycline.

2. Cerebral ischemic brain injury induction in adult mice

A. Bilateral common carotid artery occlusion (BCCAO)

Both reprogrammable mice and C57BL/6J mice were anesthetized via intraperitoneal injection of ketamine (100 mg/kg) and xylazine (10 mg/kg). Transient cerebral ischemia was induced by bilateral common carotid artery occlusion (BCCAO) for 20 minutes using vascular clamps as previously described (Figure 2).[58,59] Sham animals underwent surgical process without the occlusion of blood vessels.

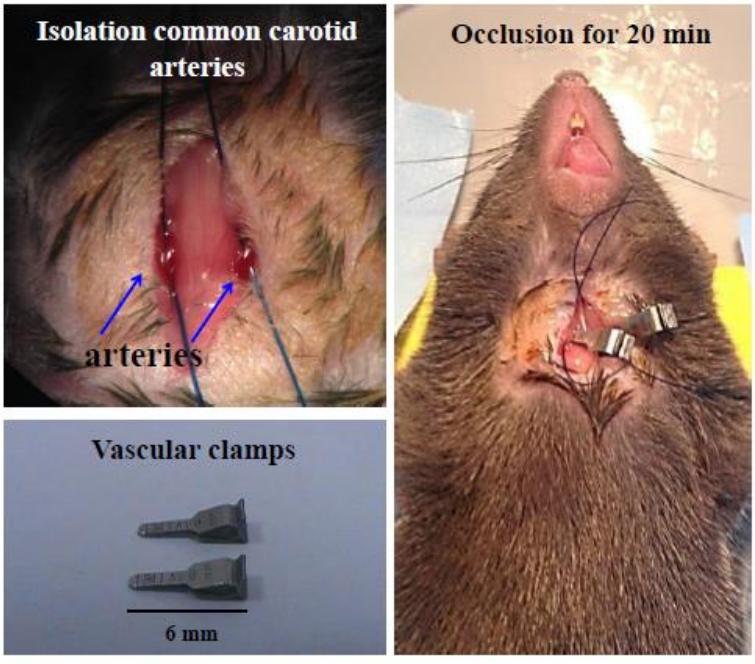

Figure 2. Bilateral common carotid artery occlusion (BCCAO) mouse model. Transient global cerebral ischemia has been caused by occlusion of bilateral carotid artery. In 8~16-week-old mice, ischemic brain damage is induced by bilateral common carotid artery occlusion for 20 minutes. 20 minutes of ischemic insult leads to neuronal death in the striatum and cortex in rodent.

B. Hypoxic-ischemic (HI) brain injury

Reprogrammable mice were anesthetized by intraperitoneal injection of ketamine (100 mg/kg) and xylazine (10 mg/kg). First, ischemic brain injury was induced by permanent ligation of the right carotid artery and mice were kept in a warm chamber until completely awake. They were then exposed to hypoxic condition (8% O_2 and 92% N_2) for 45 minutes (Figure 3).

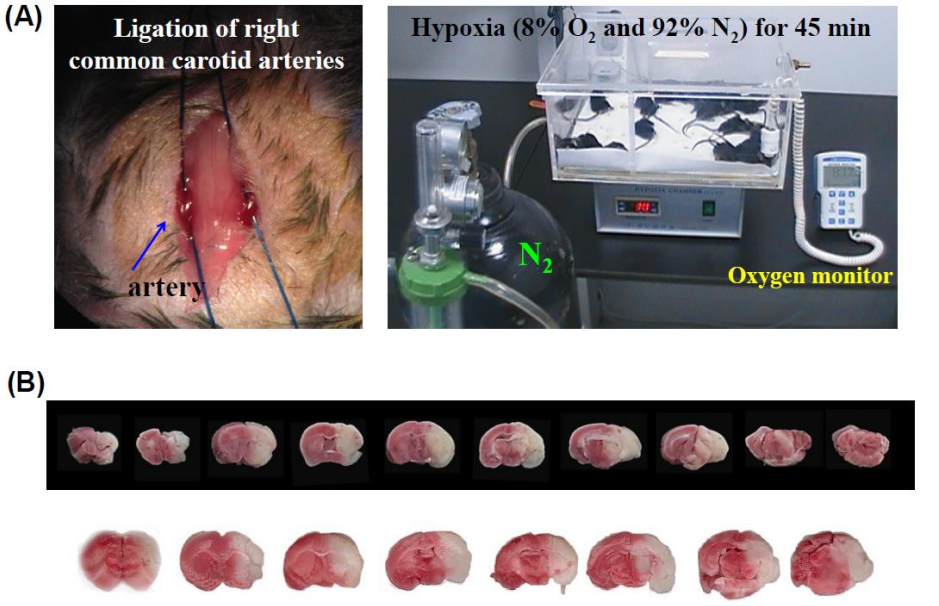

Figure 3. Hypoxic-ischemic (HI) stroke mouse model. (A) Focal ischemia has been caused by permanent ligation of unilateral carotid artery and exposure to hypoxic condition (8% O_2 and 92% N_2) for 45 minutes. (B) Brain damage is shown using TTC strain at 1 day after hypoxic-ischemic brain damage (right side). TTC, 2, 3, 5-triphenyltetrazolium chloride.

3. Doxycycline infusion using osmotic pump in the brain

After a recovery period, the brains of all the mice were injected with an osmotic pump (Figure 4A, B). In the BCCAO model, mice were continuously injected either with 1) DOX-1 (1 μg/ml) or DOX-100 (100 μg/ml) concentrations of doxycycline (No. 631311, Clontech, CA, USA) or 2) PBS (solvent control) into the lateral ventricle using a micro-osmotic pump (Alzet 1007D; 100 μl volume, Cupertino, CA, USA) at a speed of 0.5 μl/h (12 ng or 1,200 ng doxycycline/day). The infusion cannula (Brain Infusion Kit 3; 1-3 mm; Durect Corp., Cupertino, CA, USA) was inserted into the lateral ventricle using stereotaxic coordinates (AP + 0.3mm from Bregma; ML - 0.7 mm from Bregma; DV - 2.0 mm from dura).

In the adult HI model, doxycycline was injected via two routes into the lateral ventricle and striatum using stereotaxic coordinates (AP + 0.4mm from Bregma; ML - 1.9 mm from Bregma; DV - 3.3 mm from dura). Finally, to confirm the effect of extremely high dose of doxycycline (high expression of reprogramming factors), 1,000 μg/ml of doxycycline was injected into both the lateral ventricle and the striatum, and the connected osmotic pump was placed in the dorsal subcutaneous tissue (Figure 4C, D).

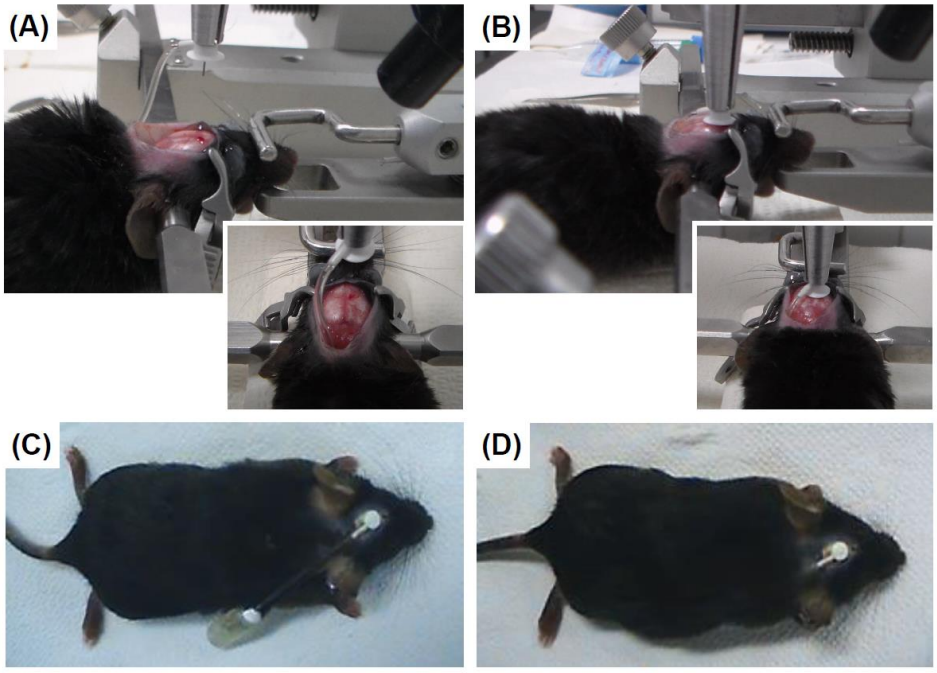

Figure 4. Infusion of doxycycline in the brain using osmotic pump. Micro-osmotic pump was injected into the lateral ventricle or striatum. (A, B) The infusion cannula was inserted using stereotaxic coordinates into the target region of the brain (lateral ventricle or striatum), and (C, D) the connected osmotic pump was placed in the dorsal subcutaneous tissue.

4. 5-bromo-2-deoxyuridine (BrdU) injection

Mice used for histology evaluation were given a daily intraperitoneal injection of 5-bromo-2-deoxyuridine (BrdU; 50 mg/kg, Sigma-Aldrich, St. Louis, MO, USA) in order to track newly generated cells for 12 days, beginning after stereotaxic surgery. Some mice for the molecular study were examined without having received BrdU injection.

5. Neurobehavioral assessment

All mice were tested to determine their functional ability. In the BCCAO model, the rotarod and ladder walking tests were impelemented at 1, 14, and 28 days after surgery (Figure 5). Two additional tests—the scylinder and grip strength tests—were used in the adult HI model 1~3 days after the HI injury, and 14 and 28 days after pump infusion (Figure 6).

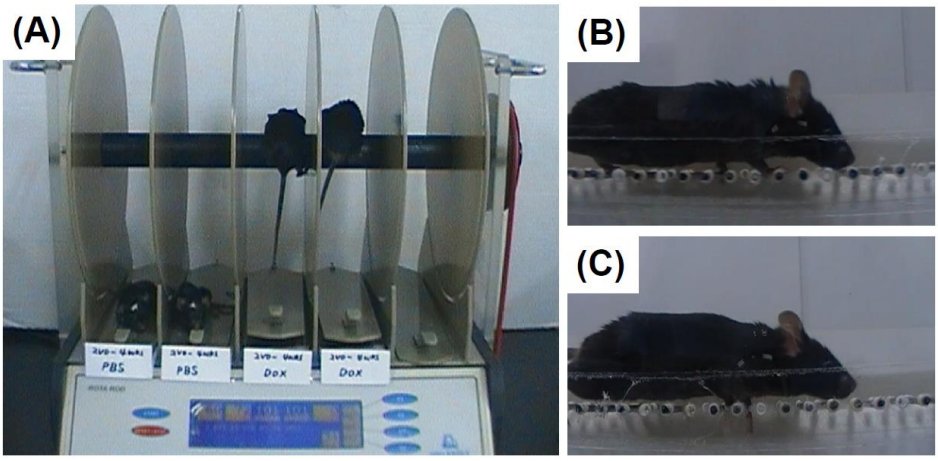

Figure 5. Behavioral assessment in BCCAO mouse model. (A-C) Representative pictures of the rotarod test and the ladder walking test. After the induction of transient global cerebral ischemia, the doxycycline-inducible reprogrammable mice were infused with doxycycline or phosphate buffered saline (control buffer) into the lateral ventricle for 7 days. (A) Mice were subjected to the rotarod test at accelerating speed (4-80 rpm) and constant speed (32 rpm). (B, C) For the ladder walking test, the mice were required to walk a distance of 1 m three times on a horizontal ladder with unevenly spaced metal rungs. The number of slips from the transverse rungs with each forelimb was measured by videotape analysis.

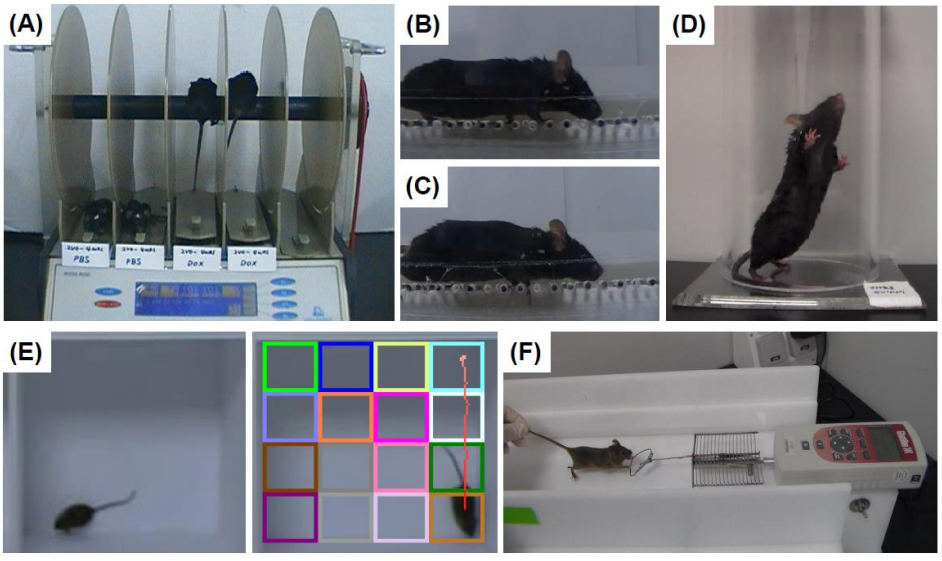

Figure 6. Neurobehavioral evaluation in HI mouse model. (A-E) Representative pictures of the rotarod test, ladder-walking test, cylinder test, open field test and grip strength test. After the induction of hypoxic-ischemic brain injury, the doxycycline-inducible reprogrammable mice were infused with doxycycline or phosphate buffered saline (control buffer) into the lateral ventricle or the striatum for 7 days. (A) Mice were subjected to the rotarod test at accelerating speed (4-80 rpm) and constant speed (32 rpm). (B-D) For assessing asymmetry, the mice were performed ladder walking test and cylinder test. The number of impaired forelimb was measured by videotape analysis. (E) Openfield test was used to assess locomotor activity and anxiety behavior. (F) Grip strength has been expressed muscle power with peak force was automatically registered in gram-force by the apparatus.

A. Rotarod test

The rotarod (No. 47600; UGO Basile, Comerio, VA, Italy) test was used to assess motor coordination and balance, using both constant speed (32 rpm) and accelerating speed (4~80 rpm) paradigms. The latency period before mice fell from the rod was measured twice during each test, and if the interval between two recorded scores was more than 60 seconds, rotarod duration was measured once more. Individual tests were terminated at a maximum latency of 300 seconds.

B. Ladder walking test

For the ladder walking test, mice were required to walk three times along a 1 m horizontal ladder with unevenly spaced metal rungs (Jeung Do B&P, Seoul, Korea). The number of slips from the transverse rungs with each forelimb was measured by videotape analysis. The percentage of slips on the transverse rungs of the ladder relative to the total number of steps taken was calculated.

The difference (Δ) in the percentage of slips on the transverse rungs of the ladder relative to the total number of steps taken by the hemiplegic forelimbs compared to the preoperative evaluation was calculated.

C. Cylinder test

A cylinder test was performed to evaluate the functional asymmetry resulting from a unilateral brain lesion and consequent hemiplegia. In the cylinder test, the number of times each forelimb contacted the cylinder wall as the mouse reared on its hind limbs was evaluated over a period of 5 minutes. The percentage of cylinder wall contacts with the hemiplegic forelimb was determined using the following formula.[16]

$$\frac{\left\{\#\ contacts\ with\ contralateral\ limb+\frac{1}{2}(\#\ contacts\ with\ both\ limbs)\right\}}{\#\ contacts\ with\ ipsilateral\ limb+\#\ contacts\ with\ contralateral\ limb+\#\ contacts\ with\ both\ limb} \times 100\ (\%)$$

The difference (Δ) in the percentage of cylinder wall contacts by the contralateral limb relative to the preoperative evaluation was calculated.

D. Grip strength test

A grip strength test was performed using the SDI Grip Strength System (San Diego Instruments Inc., San Diego, CA, USA), which includes a push-pull strain gauge. A triangular piece of metal wire 2 mm in diameter was used as the grip bar. Each animal was held near the base of its tail and was moved in close proximity to the bar until the animal could grip the bar with its forepaws. Peak force was automatically registered in gram-force by the apparatus. The mean peak force of three trials was used for analysis.[60]

E. Open field test

Activity monitoring was conducted in a square-shaped area measuring 30 × 30 × 30 cm. Mice were placed individually into the arena and monitored with a video camera.

The apparatus was cleaned with 70% alcohol and air-dried prior to the commencement of each trial for every mouse. The resulting data were analyzed using the video tracking system Smart Vision 2.5.21 (Panlab, Barcelona, Spain).

In the tracking system, the openfield test box is divided into 16 spaces (4 × 4). Four squares located in the central area, four corner squares (top-left, top-right, bottom-left, and bottom-right) and the remaining squares in the side were defined as the central zone (CZ), the corner zone (C), and the side zone (S), respectively. The distance of movement was assessed for 10 minutes.

6. Isolation of mouse embryonic fibroblasts (MEFs)

MEFs were isolated from 13.5-day old embryos in uteri of reprogrammable mice as previously described.[57] Embryo bodies without the head and visceral tissues were isolated from the embryos which were washed with phosphate-

buffered saline (PBS). The bodies were minced using autoclaved scissors and then collected in a 15-ml tube by passing them through a syringe with a 26-gauge needle 3-4 times. The tube was centrifuged at 1,000 rpm for 5 minutes at 4°C. The minced tissues were then transferred into a new 15-ml tube with 7-8 ml PBS. after suctioning PBS, tissues were collected by centrifugation (1,000 rpm for 5 minutes at 4°C) and resuspended in 7-8 ml of fresh medium (DMEM containing 10% FBS). After centrifugation (1,000 rpm for 5 minutes at 4°C), the media were discarded, and resuspended tissues were seeded with 13-ml fresh medium in 75-T flask. The flask was maintained in the culture medium until the MEFs grew up in the incubator (5% CO_2, 37°C).

7. Cell culture

MEFs seeded at a density of 1 x 10^4 cells/well in 6-well plates were cultured in Dulbecco's modified Eagle's medium (DMEM; Gibco Invitrogen, Carlsbad, CA, USA) supplemented with 10% fetal bovine serum (FBS; Gibco Invitrogen, Carlsbad, CA, USA) and 1% antibiotics (penicillin streptomycin; Gibco Invitrogen). MEFs were treated daily with various doses of doxycycline (10, 100, 500, 1,000 ng/ml) for 7 days and subjected to RT-PCR.

8. Immunohistochemistry

The animals were euthanized and perfused with 4% paraformaldehyde (PFA). The harvested brain tissues were cryosectioned at 16-μm thickness, and immunohistochemistry staining was performed on 4 sections over a range of 128 μm. The sections were stained with primary antibodies against BrdU (1:200, Abcam, Cambridge, UK), βIII-tubulin (1:400, Covance, Princeton, NJ), GFAP (1:400, Abcam), Nestin (1:400, Abcam), NeuN (1:400, Millipore), CS-56 (1:200, Abcam), CD31 (1:200, BD Bioscience, San jose, CA), and C3 (1:100, Abcam), as well as with secondary antibodies such as Alexa Fluor® 488 goat anti-Rat (1:400, Invirogen, Carlsbad, CA), Alexa Fluor® 568 goat anti-Rabbit (1:400,

Invitrogen), and Alexa Fluor® 594 goat anti-Mouse (1:400, Invitrogen). The sections were then mounted on glass slides with a fluorescent mounting medium containing 4',6- diamidino-2-phenylindole (DAPI; Vectorshield, Vector, Burlingame, CA). The stained sections were analyzed using confocal microscopy (LSM700, Zeiss, Gottingen, Germany) and the MetaMorph Imaging System (Molecular Device, Sunnyvale, CA). Blood vessel density was evaluated using a fluorescent microscope (BS51, Olympus, Tokyo, Japan) and the MetaMorph Imaging System. Images of glial scarring were taken using a fluorescent microscope (Axio Imager M2, Zeiss), and the density was evaluated using ZEN Imaging Software (Blue edition, Zeiss).

9. 2, 3, 5-triphenyltetrazolium chloride (TTC) staining

Infarct regions were confirmed using 2, 3, 5-triphenyltetrazolium chloride (Sigma) staining. At 1 day after BCCAO or HI injury, brains were sectioned into 2.0 mm coronal sections using a mouse brain matrix. The sections were incubated in 2% TTC at 37°C for 20 minutes. The brain sections were washed in PBS and then stored in 4% PFA in a 4°C refrigerator. The sections were photographed with a digital camera.

10. RNA extraction and cDNA synthesis

Total RNA was extracted from the MEFs or from the tissue samples using Trizol (Invitrogen Life Technologies, Carlsbad, CA, USA) according to the manufacturers' protocols.[61] The Agilent 2100 Bioanalyzer (Agilent Technologies, Palo Alto, CA, USA), with an A260/A280 ratio for quality control analysis, was used to evaluate the purity of the RNA extracted from brain tissues. 1 μg of purified total RNA was used for reverse transcription into cDNA using a ReverTra Ace® qPCR TR master Mix with gDNA remover (ToyoBo, Tokyo, Japan).

11. Reverse transcription-polymerase chain reaction (RT-PCR)

cDNA was subjected to PCR using both an RT-PCR analysis kit (Bioneer, Daejeon, Korea) according to the manufacturer's instructions and a Gene Amp PCR system 9700 (Applied Biosystems/Life Technologies, Carlsbad, CA, USA). The primer sequences are described in Table 1. The thermocycler conditions were as follows: denaturation for 1 minute at 95°C, followed by 35 cycles at 95°C for 30 seconds, at 58°C for 30 seconds, and at 72°C for 30 seconds. PCR products were subjected to 1.5% agarose gel electrophoresis.

Table 1. The sequences of primers for RT-PCR

Genes	Primer sequences	
Pou5fl (Oct4)	Forward	TCTTTCCACCAGGCCCCCGGCTC
	Reverse	TGCGGGCGGACATGGGGAGATCC
Sox2	Forward	TAGAGCTAGACTCCGGGCGATGA
	Reverse	TTGCCTTAAACAAGACCACGAAA
Gapdh	Forward	CAAGGTCATCCATGACAACTTTG
	Reverse	GTCCACCACCCTGTTGCTGTAG

12. Quantitative real-time polymerase chain reaction (qRT-PCR)

1μL of cDNA in a total volume of 20 μL was used in the following reaction. The qRT-PCR was performed in triplicate on a LightCycler 480 (Roche Applied Science, Mannheim, Germany) using the LightCycler 480 SYBR Green master mix (Roche Applied Science). The thermocycler conditions were as follows: amplifications were performed beginning with a 300-second template preincubation step at 95°C, followed by 40 cycles at 95°C for 5 seconds, at 60°C for 20 seconds, and at 95°C for 15 seconds. Melting curve analysis began at 95°C for 15 seconds, followed by 1 minute at 60°C. The specificity of the amplification product was confirmed by an examination of the melting curve, which showed a distinct single sharp peak with the expected Tm for all samples. A distinct single peak indicates that a single DNA sequence was amplified during qRT-PCR. Glyceraldehyde-3-phosphate dehydrogenase (Gapdh) was used as an internal control. The expression of each gene of interest was obtained using the $2^{-\Delta\Delta Ct}$ method. The primer sequences for qRT-PCR are described in Table 2.

Table 2. The sequences of primers for qRT-PCR

Genes	Primer sequences	
C3	Forward	GAGAGCGAAGAGACCATCGTA
	Reverse	TGTGCCCCTCCTTATCTGAGT
C4a	Forward	GCATGGAGCGCCTACGAA
	Reverse	CTTGCCATTGCGCCAGATAC
C4b	Forward	CACACCTTGCCCGAAACAAC
	Reverse	TGCTTTTGGACAGGCTCACA
C3ar1	Forward	TACACTGAACGCTGACGCTT
	Reverse	TGGTTATTGCCATCAGCGGT
C1qa	Forward	AAGGACTGAAGGGCGTGAAA
	Reverse	CACTGCACAGATGAAGCGAC
C1qb	Forward	AAGGCGATTCTGGGGACTAC
	Reverse	GCGTGGCTCATAGTTCTCGT
C1qc	Forward	TGGAGGGCCGATACAAACAG
	Reverse	AACTTCCCTGTGCTTGGGTT
GFAP	Forward	TTGCTGGAGGGCGAAGAAAA
	Reverse	CATCCCGCATCTCCACAGTC
Vimentin	Forward	TTCTCTGGCACGTCTTGACC
	Reverse	CTTTCATACTGCTGGCGCAC
S100β	Forward	TGGTTGCCCTCATTGATGTCTT
	Reverse	TTCGTCCAGCGTCTCCATCA
Gapdh	Forward	CAAGGTCATCCATGACAACTTTG
	Reverse	GTCCACCACCCTGTTGCTGTAG

13. Transcriptome screening

mRNA sequencing was processed for transcriptome analysis by Macrogen, Inc. (Seoul, Korea) as previously described.[61,62]

Transcripts with cut offs at fold change ≥1.5 and statistically significant P-values ≤ 0.05 were considered and included in downstream analysis.

14. Statistical analysis

All data were expressed as means ± S.E.M. The variables between groups were analyzed using one-way analysis of variance (ANOVA) followed by a post-hoc Bonferroni comparison using the SPSS statistics software (IBM corporation, Armonk, NY; version 20.0). Comparison of variables between two groups was performed using Student's t-test. A P value < 0.05 was considered statistically significant.

III. RESULTS

1. Bilateral common carotid artery occlusion (BCCAO) model

In BCCAO model, this study investigated histological and behavioral changes evoked by doxycycline (DOX) administered in two concentrations (DOX-1, DOX-100) to reprogrammable mice in order to elucidate the mechanism behind the potential therapeutic effects of the reprogramming factors. The experimental design for the BCCAO mouse model is described in Figure 7.

A. *In vitro* reprogramming factor expression led to changes in the morphology of mouse embryonic fibroblasts (MEFs)

To confirm reprogramming capacity in vitro, MEFs were isolated from the reprogrammable mice to express reprogramming factors by doxycycline. These cells changed their morphology beginning on day threes following the expression of reprogramming factors via doxycycline administration (500 μg/ml) (Figure 8).

MEFs were treated with several concentrations of doxycycline (10, 100, 500, and 1,000 ng/ml) for 7 days. Expression levels of the reprogramming factors Pou5f1 (Oct4) and Sox2 were determined by RT-PCR. To determine whether doxycycline induced expression of reprogramming factors *in vivo*, expression of Sox2 was measured using qRT-PCR at 3 days after the infusion of doxycycline. The results showed that Sox2 expression in the striatum increased in a dose-dependent manner in mice treated with DOX-100 (100 μg/ml) compared with other groups ($P < 0.05$) (Figure 9).

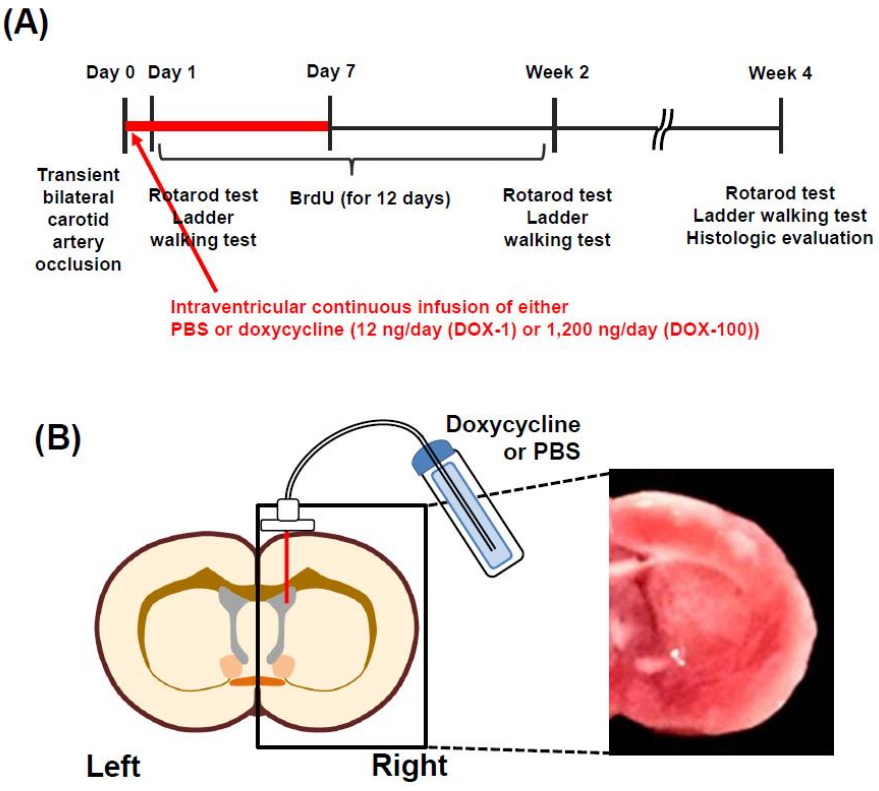

Figure 7. Study design and doxycycline injection. (A) Study design. Transient cerebral ischemia was induced by 20 minutes bilateral common carotid artery occlusion (two vessel occlusion) in the doxycycline (DOX)-inducible reprogrammable mice. Thereafter, DOX (DOX-1, 1 μg/ml; DOX-100, 100 μg/ml) or phosphate buffered saline (PBS, control buffer) was continuously infused into the right lateral ventricle via an osmotic pump over 7 days and BrdU was daily injected for 12 days. Behavioral tests such as the rotarod and ladder walking tests were performed. Four weeks after the cerebral ischemia induction, the mice were euthanized and histologically analyzed. (B) DOX injection into the lateral ventricle via an osmotic pump (left side) to infuse low (12 ng/day, DOX-1) or high (1,200 ng/day, DOX-100). Brain damage is shown using TTC strain at 1 day after ischemic injury (right side).

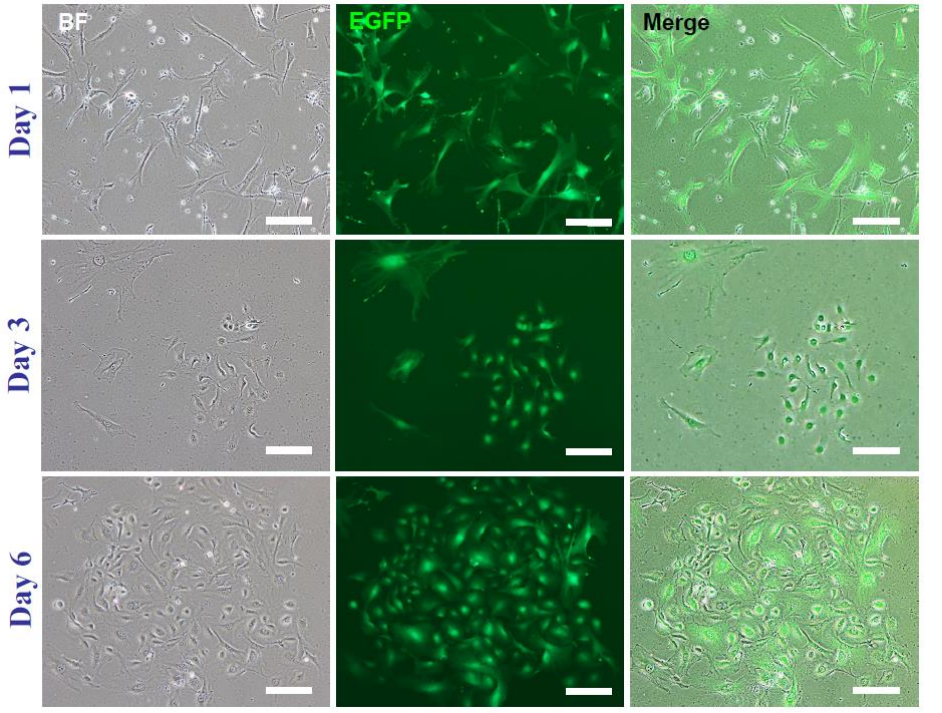

Figure 8. MEFs derived from reprogrammable mice was changed morphology via expression of reprogramming factors. To confirm reprogramming capacity *in vitro*, the fibroblast was isolated from reprogrammable mice. Mouse embryonic fibroblasts (MEFs) derived from mice to expression reprogramming factors by doxycycline (500 μg/ml) were observed morphological changes at Day 3 and Day 6 after expression of reprogramming factors. Scale bar = 200 μm

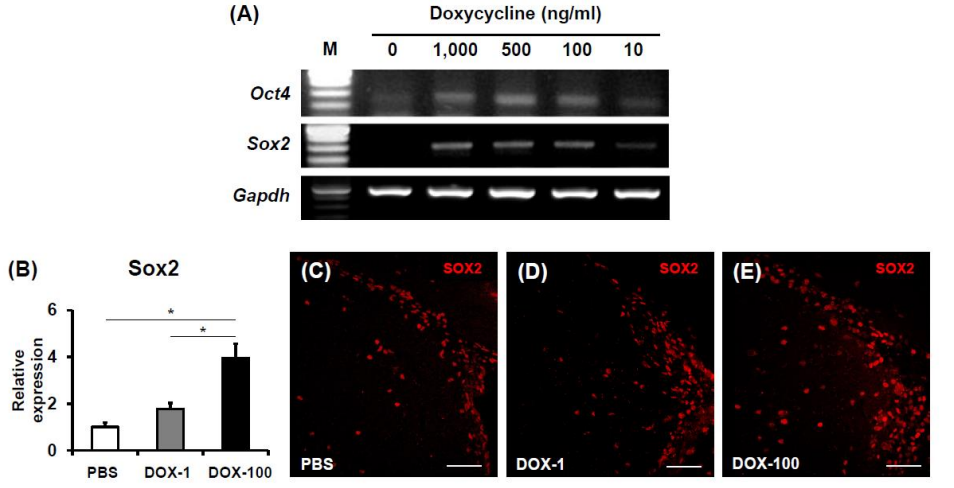

Figure 9. *In vitro* and *in vivo* reprogramming factor were expressed by doxycycline. (A) Mouse embryonic fibroblasts isolated from the reprogrammable mice were treated with several concentrations of doxycycline (10, 100, 500, and 1,000 ng/ml) for 7 days. Expression levels of the reprogramming factors, Pou5f1 (Oct4) and Sox2, were determined by RT-PCR using Gapdh as the internal control. (B) Expression of Sox2 evaluated by qRT-PCR significantly increased in the striatum of mice treated with DOX-100 (100 μg/ml) compared with the other groups in a dose-dependent manner (n = 4/group; *P < 0.05, one-way ANOVA followed by a post-hoc Bonferroni comparison). mean + SEM. (C-E) Representative confocal microscopic images. Scale bar = 50 μm

B. *In vivo* transient expression of reprogramming factors was not involved in tumor formation

Although *in vivo* doxycycline-induced expression of reprogramming factors has been reported to cause tumor formation in epithelial tissues,[63,64] tumor-like tissues were not observed in terms of the tumor formation at 4 weeks after the initiation of one-week low-dose doxycycline infusion (Figure 10).

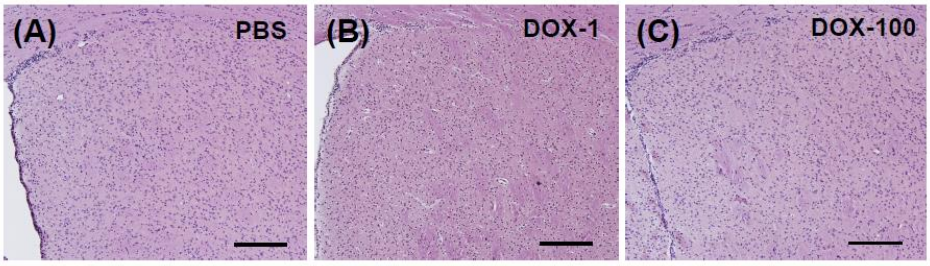

Figure 10. Tumor was not observed in brain tissue. (A-C) At 4 weeks after the initiation of DOX-100, DOX-1, or PBS infusion, brain sections were stained with hematoxylin and eosin (H&E) and observed using a microscope. Tumor-like tissue was not observed in any groups. Scale bars = 200 μm.

C. *In vivo* reprogramming factor expression increased new neural progenitors and astrocytes in the subventricular zone

To elicit expression of reprogramming factors *in vivo*, transgenic mice in which the four reprogramming factors (Oct4, Sox2, Myc, and Klf4) are expressed in a doxycycline-inducible manner were used.[57] To express the factors in damaged brain tissues *in vivo*, an osmotic pump was used to infuse low (12 ng/day, DOX-1 group) or high (1,200 ng/day, DOX-100 group) amounts of doxycycline or control buffer (PBS) into the lateral ventricles of the reprogrammable mice for 7 days beginning immediately after 20 minute-bilateral common carotid artery occlusion[58] (Figure 2).

To determine whether this *in vivo* expression enhances cell proliferation in the damaged tissue, neurogenesis and gliogenesis levels were determined in the subventricular zone, the site of the highest expected concentration of doxycycline after diffusion from the lateral ventricle. This is also the site where neural stem/progenitor cells, which contribute to regeneration, exist in the adult mammalian brain.[65,66] To label proliferating cells, BrdU was given to the mice every day for 12 days following the stereotaxic surgery. The number of $BrdU^+$ cells in the subventricular zones of mice in the DOX-100 and DOX-1 groups were 7.7 times and 4.5 times higher, respectively, than the number of of $BrdU^+$ cells in the PBS control ($P < 0.001$ and $P < 0.01$, respectively), and the number of $BrdU^+$ cells in the DOX-100 group was 1.7 times higher than in the DOX-1 group ($P < 0.01$), indicating that the presence of reprogramming factors enhances cell proliferation in the subventricular zone in a dose-dependent manner (Figure 11).

Next, to identify proliferating cells, histologic analysis was performed by double-staining with BrdU and with cell type-specific markers such as βIII-tubulin (Tuj1, a neuronal marker), GFAP (an astrocyte marker), or Nestin (a neural progenitor cell marker) in the subventricular zone. The numbers of $BrdU^+Nestin^+$cells in the DOX-100 and DOX-1 groups were 26.5 and 20.4 times higher, respectively, than in the PBS control group ($P < 0.01$ and $P < 0.05$, respectively), indicating that *in vivo* expression of reprogramming factors enhances the proliferation of neural progenitor cells. The numbers of $BrdU^+GFAP^+$ cells in the DOX-100 and DOX-1 groups were 15.2 and 10.8 times higher, respectively, than in the PBS control group ($P < 0.001$ and $P < 0.01$, respectively), suggesting that reprogramming factor expression causes a robust proliferative generation of astrocytes. However, the number of $BrdU^+$βIII-$tubulin^+$ cells was similar across all groups, suggesting that neurogenesis in the subventricular zone is not affected by the reprogramming factors (Figure 11).

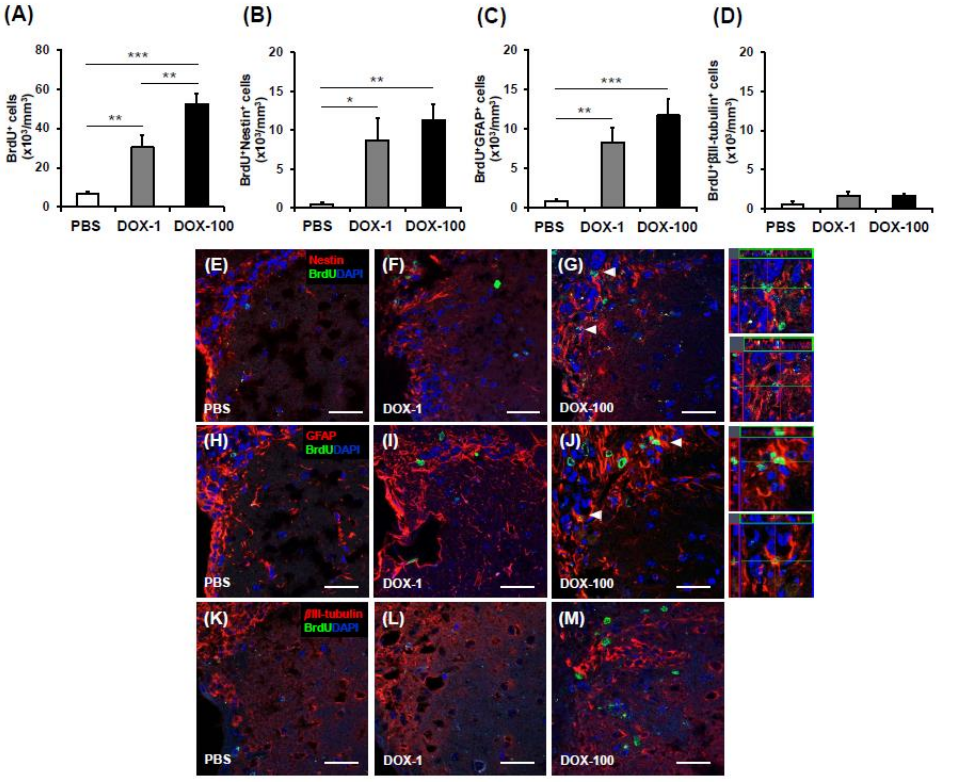

Figure 11. Increased number of newly generated neural progenitors and astrocytes induced by reprogramming factor expression in the subventricular zone. After the induction of cerebral ischemia, the doxycycline (DOX)-inducible reprogrammable mice were infused with two doses of doxycycline (DOX-1 and DOX-100) or phosphate buffered saline (PBS, control buffer) into the right lateral ventricle for 7 days. To identify newly generated cells, the mice were daily injected daily with 5-bromo-2-deoxyuridine (BrdU) for 12 days. Four weeks after ischemia induction, histologic evaluations were performed. (A) The density of $BrdU^+$ cells in the subventricular zone was significantly higher in both the DOX-100 and DOX-1 groups than in the PBS controls (n = 5/group; *P < 0.05; **P < 0.01 and ***P < 0.001, one-way ANOVA followed by a post-hoc Bonferroni comparison). (B-D) The density of newly generated neural

progenitors, astrocytes, and neurons was determined through confocal microscopy by calculating the density of cells triple positive for DAPI (blue, nuclei), BrdU (green), and cell type-specific markers such as Nestin, GFAP, and βIII-tubulin, respectively. The densities of $BrdU^+Nestin^+$ and $BrdU^+GFAP^+$ cells but not $BrdU^+$βIII-$tubulin^+$ cells in both the DOX-100 and DOX-1 groups were significantly higher than in the PBS controls. (n = 5/group; *P < 0.05; **P < 0.01 and ***P < 0.001, one-way ANOVA followed by a post-hoc Bonferroni comparison). (E-M) Representative confocal microscopic images. (G, J) Cells triple positive for DAPI, BrdU, and cell type-specific markers are indicated with white arrow heads in the right panel. Scale bars = 25 μm. mean + SEM.

D. Reprogramming factor expression increased newly generated astrocytes but not neurons or glial scar formation in the striatum

Motor performance as evaluated by the rotarod and forelimb slip tests were largely affected by striatal function. Moreover, the striatum is the second closest site to the lateral ventricle where doxycycline was infused. Furthermore, the activation of neural stem/progenitor cells in the subventricular zone through the intraventricular administration of growth factors (including BDNF) can also turn the striatum into a regenerative environment.[16,17,67] Thus, neurogenesis and gliogenesis were evaluated in the right striatum in order to determine whether *in vivo* reprogramming factor expression can similarly transform the damaged striatum into a restorative environment.

The numbers of $BrdU^+$ cells in both the DOX-100 and DOX-1 groups were 4.3 and 3.7 times higher, respectively, than in the PBS control group (P < 0.001), suggesting that doxycycline-induced reprogramming factor expression increases the number of proliferating cells in the striatum. As in the subventricular zone, the number of $BrdU^+GFAP^+$ cells in the DOX-100 group was 2.2 times higher than in the PBS control group, in which $BrdU^+GFAP^+$ cells were barely observed (P < 0.001), suggesting that reprogramming factor expression robustly increases

the number of newly generated astrocytes in the striatum. The number of $BrdU^+$βIII-$tubulin^+$ cells in the striatum was much lower than in the subventricular zone and was similar among all groups, suggesting that neurogenesis in the striatum is not altered by the expression of reprogramming factors (Figure 12A-C). In addition, levels of the glial scar marker CS-56 did not differ among the groups, suggesting that the astrocytes that are newly generated by *in vivo* reprogramming factor expression do not increase the detrimental glial scar formation that inhibits neuroregeneration after ischemic brain damage (Figure 12D).

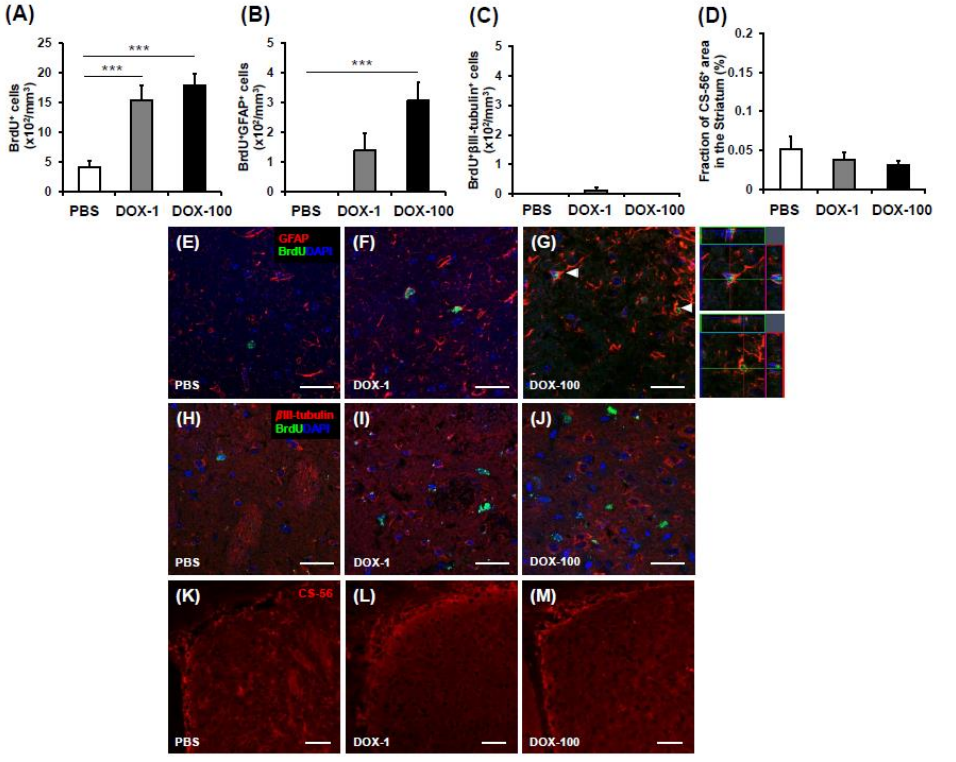

Figure 12. Reprogramming factor expression increased the number of newly generated astrocytes in the striatum. (A) The densities of $BrdU^+$ cells in the striatum of both DOX-100 and DOX-1 groups were significantly higher than in the PBS controls (n = 5/group; **P < 0.01; ***P < 0.001, one-way ANOVA followed by a post-hoc Bonferroni comparison). (B, C) The density of newly generated astrocytes and neurons was determined through confocal microscopy by calculating the density of cells triple positive for DAPI (blue, nuclei), BrdU (green), and cell type-specific markers such as GFAP and βIII-tubulin, respectively. The density of $BrdU^+GFAP^+$ cells, but not BrdU+βIII-tubulin+ cells, was significantly higher in the DOX-100 group than in the DOX-1 and PBS groups (n = 5/group; ***P < 0.001, one-way ANOVA followed by a post-hoc Bonferroni comparison). (D) The density of area positive for CS-56, a marker of

glial scar. The area of CS-56 staining did not differ among the groups (n = 5/group). (E-J) Representative confocal microscopic images of $BrdU^+GFAP^+$ cells and $BrdU^+\beta III\text{-}tubulin^+$ cells in the striatum. (G) Three dimensional images of cells triple positive for DAPI, BrdU, and GFAP are indicated with arrow heads in the right panel. Scale bars = 25 μm. (K-P) Representative fluorescent microscopic images of staining for CS-56. Scale bars = 50 μm. mean + SEM. CS-56, chondroitin sulfate-56.

To determine whether the density of the astrocytes generated through proliferation varies in regions within the striatum, the striatum was divided into five regions, and the densities of $BrdU^+$ and $BrdU^+GFAP^+$ cells in each region were evaluated. In the PBS group, the densities of $BrdU^+$ cells were comparable between regions, and the density of $BrdU^+GFAP^+$ cells were below the detection range in all regions. In both the DOX-1 and DOX-100 groups, the densities of $BrdU^+$ and $BrdU^+GFAP^+$ cells showed a tendency to be high when the analyzed regions were closer to the lateral ventricle where doxycycline was infused. In line with this regional tendency, the density of $BrdU^+$ cells were significantly higher in region 1, which is closest to the lateral ventricle, in the DOX-100 and DOX-1 groups. Furthermore, the density of the $BrdU^+GFAP^+$ cells in region 1 in the DOX-100 group was significantly higher than in regions 4 and 5 ($P < 0.05$). Likewise, in regions 1, 2, and 3, the densities of $BrdU^+$ cells in the DOX-100 and DOX-1 groups were significantly higher than in the PBS group. The densities of $BrdU^+GFAP^+$ cells in region 1 in the DOX-100 and DOX-1 groups were significantly higher than in the PBS group ($P < 0.01$ and $P < 0.05$, respectively) (Figure 13). Taken together, these data indicate that the densities of all proliferated cells and proliferated astrocytes were significantly higher in the striatum regions closer to the lateral ventricle.

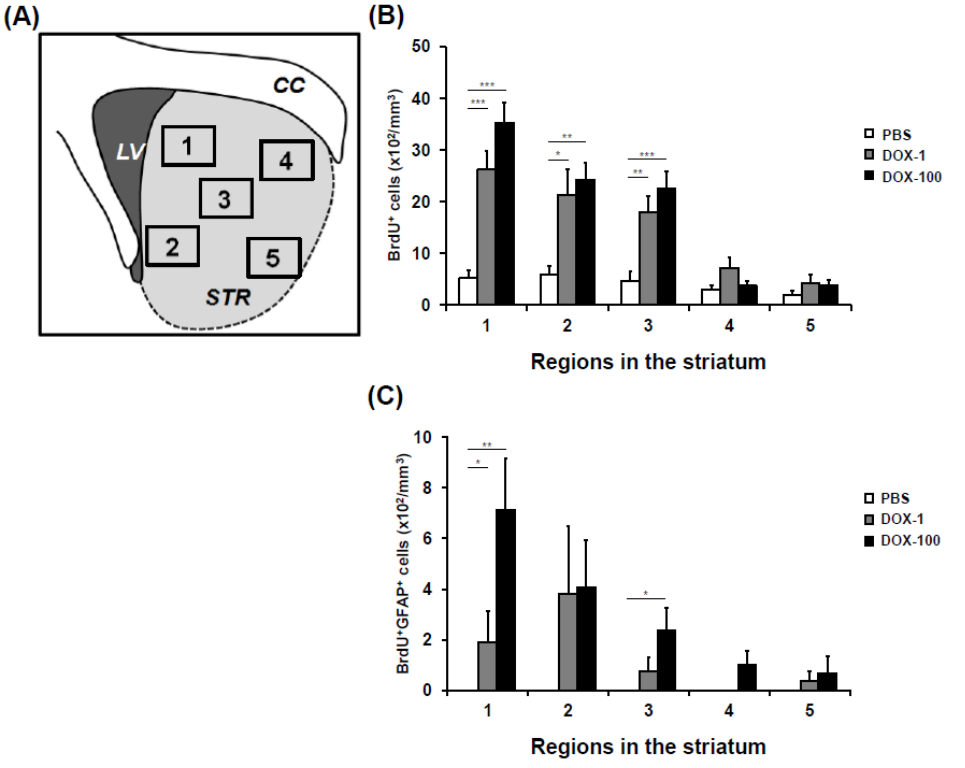

Figure 13. Regional density of BrdU$^+$ and BrdU$^+$GFAP$^+$ cells in the striatum. (A) The striatum was divided into five regions and each region was subjected to analysis. (B, C) Regional analysis. The density of BrdU$^+$ and BrdU$^+$GFAP$^+$ cells in the right striatum from mice in the DOX group showed a tendency to decrease as the distance between the lateral ventricle and analyzed regions increased. The density of BrdU$^+$ cells was comparable between the regions in (B). (B) The densities of BrdU$^+$ cells in regions 1, 2 and 3 of the DOX-100 and DOX-1 groups were significantly higher than in the PBS group (n = 5/group; *P < 0.05; **P < 0.01 and ***P < 0.001, one-way ANOVA followed by a post-hoc Bonferroni comparison). (C) The density of BrdU$^+$GFAP$^+$ cells in region 1 in the DOX-100 and DOX-1 groups were significantly higher than in the PBS group (n = 5/group;

**P < 0.01 and *P < 0.05, respectively, one-way ANOVA followed by a post-hoc Bonferroni comparison). mean + SEM.

E. *In vivo* reprogramming factor expression enhanced angiogenesis

Angiogenesis is a critical process for the recovery of ischemic tissue. Blood vessel density was evaluated in the striatum by staining the tissue with an anti-CD31 antibody, which recognizes a representative endothelial cell marker. The number of $CD31^+$ capillaries in the DOX-100 group was 1.2 and 1.1 times higher than in the PBS control and DOX-1 groups, respectively ($P < 0.001$ and $P < 0.05$), indicating that the level of angiogenesis was highest in the DOX-100 group. Next, a potential mechanism underlying this increased angiogenesis was identified in the ischemic brain. Given that astrocytes play crucial roles in brain neovascularization,[68,69] the increased angiogenesis induced by reprogramming factor expression might be, at least in part, attributable to the enhanced proliferative generation of astrocytes. Furthermore, the use of confocal microscopy revealed that $CD31^+$ blood vessels were frequently surrounded by astrocytes (Figure 14)

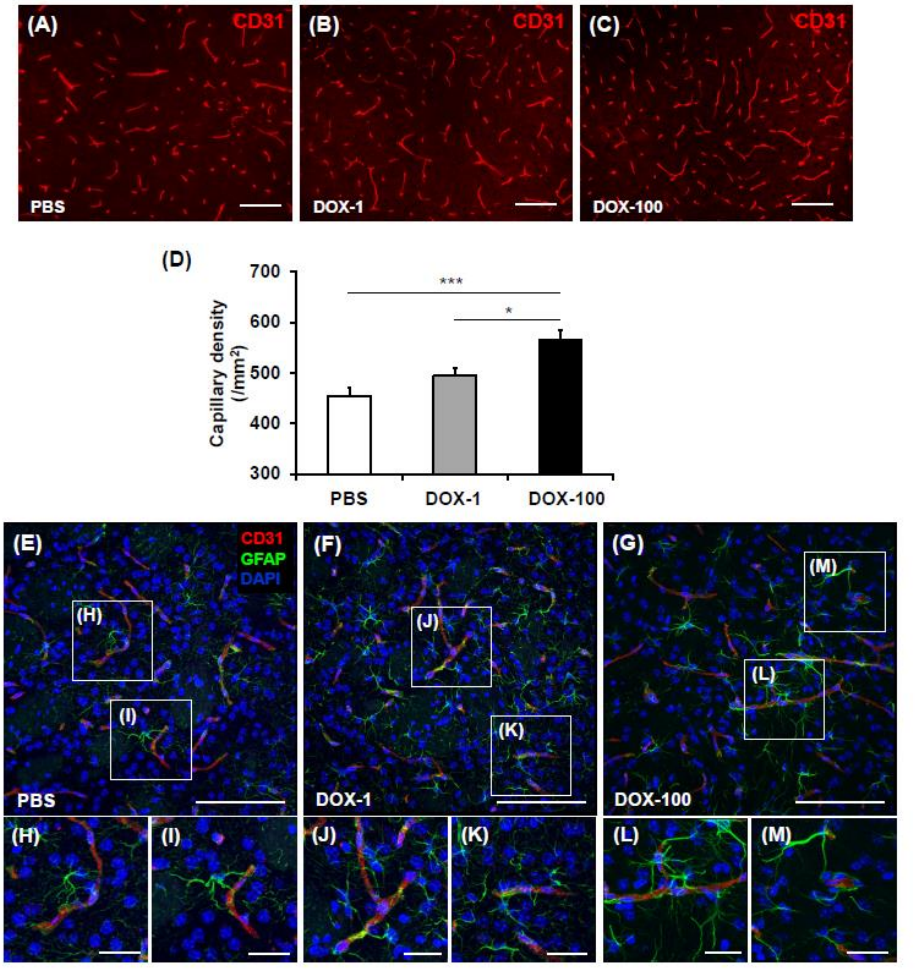

Figure 14. Angiogenesis was enhanced by reprogramming factor expression in the striatum. Four weeks after ischemia induction, the blood vessel density was determined by immunofluorescent staining against CD31. (A-C) Representative fluorescent microscopic images. Scale bar = 100 μm. (D) The $CD31^+$ area (blood vessel-occupying region) was significantly larger and the density of $CD31^+$ capillaries in the striatum was significantly higher in DOX-100 group than in both the DOX-1 and PBS controls. (n = 6/group; ***P < 0.001 and *P < 0.05 respectively, one-way ANOVA followed by a post-hoc Bonferroni

comparison). (E-M) Confocal microscopic pictures showing blood vessels close to astrocytes. $CD31^+$ endothelial cells lining blood vessels are surrounded with $GFAP^+$ astrocytes in PBS, DOX-1, and DOX-100 groups. Scale bar = 25 μm. mean + SEM. CD31, cluster of differentiation 31.

F. *In vivo* reprogramming factor expression increased neuronal survival and synaptic plasticity

Astrocytes play a crucial role in neuroprotection by releasing several growth factors and cytokines.[70,71] To test whether newly generated astrocytes and angiogenesis induced by *in vivo* reprogramming factor expression can increase neuronal survival and synaptic plasticity, the expression of the mature neuronal marker NeuN and synaptic markers such as synaptophysin and PSD95 were evaluated by qRT-PCR. The results of this analysis showed that the expression of striatal NeuN increased significantly in mice treated with DOX-100 compared with mice in the PBS control group ($P < 0.05$). Similarly, expression of synaptophysin and PSD 95 in the striatum significantly increased in the DOX-100 group compared with the DOX-1 and PBS groups ($P < 0.01$ and $P < 0.001$). In addition, the number of $NeuN^+$ cells (/mm^3) and the fraction of area in the striatum were counted using an anti-NeuN antibody. The number of $NeuN^+$ cells (/mm3) and the fraction of $NenN^+$ in the striatum (%) were significantly higher in mice treated with DOX-100 (Figure 15)

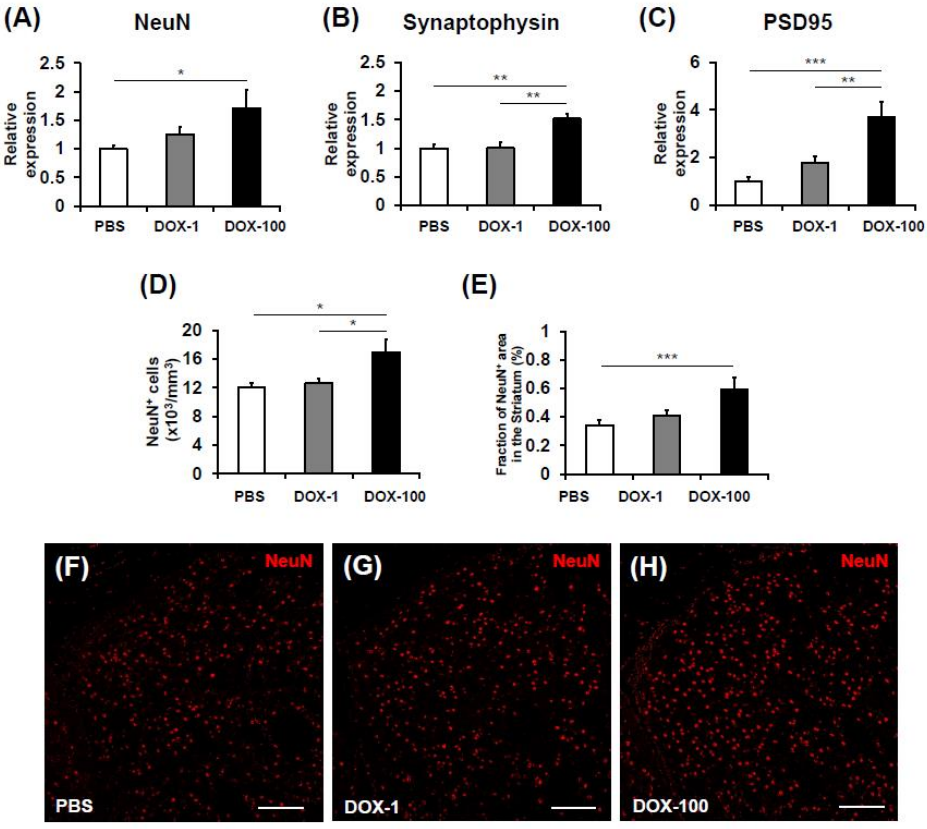

Figure 15. ***In vivo*** **reprogramming factor expression enhanced neural survival and synaptic plasticity.** Gene expression of markers of neural survival and synaptic plasticity was evaluated by qRT-PCR. (A) Expression of striatal NeuN significantly increased in mice treated with DOX-100 compared to the PBS control group (n = 4/group; *P < 0.05, one-way ANOVA followed by a post-hoc Bonferroni comparison). (B, C) Similarly, expression of synaptic markers such as synaptophysin and PSD95 significantly increased in the striatum in the DOX-100 group compared to the DOX-1 and PBS groups (n = 4/group; **P < 0.01, ***P < 0.001, one-way ANOVA followed by a post-hoc Bonferroni comparison). (D, E) The number of $NeuN^+$ cells (/mm^3) and the fraction of area that was $NeuN^+$ in the striatum (%) were significantly higher in mice treated with DOX-100 (n =

5/group; *P < 0.05, ***P < 0.001, one-way ANOVA followed by a post-hoc Bonferroni comparison). (F-H) Representative microscopic images of $NeuN^+$ cells in the striatum. Scale bar = 100 μm. mean + SEM.

G. *In vivo* reprogramming factor expression facilitated behavioral functional restoration after ischemic brain injury

To determine whether *in vivo* reprogramming factor expression enhances functional recovery in the ischemic brain damage model, neurobehavioral functions were evaluated by rotarod and ladder walking tests at 2 and 4 weeks after doxycycline infusion. Rotarod tests with constant (32 rpm) speed showed that the latency periods before falling in the DOX-100 group were 262.4 ± 18.8 and 241.1 ± 23.7 seconds at 2 and 4 weeks post-treatment, respectively, which was 4.0 and 5.1 times higher, respectively, than in the PBS control group (64.9 ± 26.9 and 46.6 ± 15.1 seconds, respectively) (P < 0.001). Rotarod tests with accelerating speed (4~80 rpm) also revealed that the latency periods before falling in the DOX-100 group were 150.4 ± 5.0 and 140.7 ± 7.9 seconds at 2 and 4 weeks post-treatment, which was 1.5 times and 1.8 times higher, respectively, than in the PBS control group (100.4 ± 14.7 and 80.1 ± 15.4 seconds, respectively) (P < 0.05 and P < 0.01). These results further confirm that reprogramming factor expression enhances the improvement of motor function (Figure 16A, B)

Ladder walking tests, which evaluate fine motor coordination, showed that forelimb slip rates relative to total steps in the DOX-100 group at 2 and 4 weeks post-treatment were 3.3 ± 0.6% and 2.5 ± 0.4%, respectively, which are 2.0 and 3.0 times lower, respectively, than in the PBS group (6.7 ± 1.5% and 7.5 ± 1.3%, respectively; P < 0.05 and P < 0.01, respectively). In addition, the forelimb slip rate in the DOX-1 group at 4 weeks post-treatment was 4.3 ± 0.8%, which was 1.8 times lower than in the PBS group (P < 0.05), indicating that *in vivo* reprogramming factor expression can enhance the recovery of coordinated motor function in this cerebral ischemia model (Figure 16C).

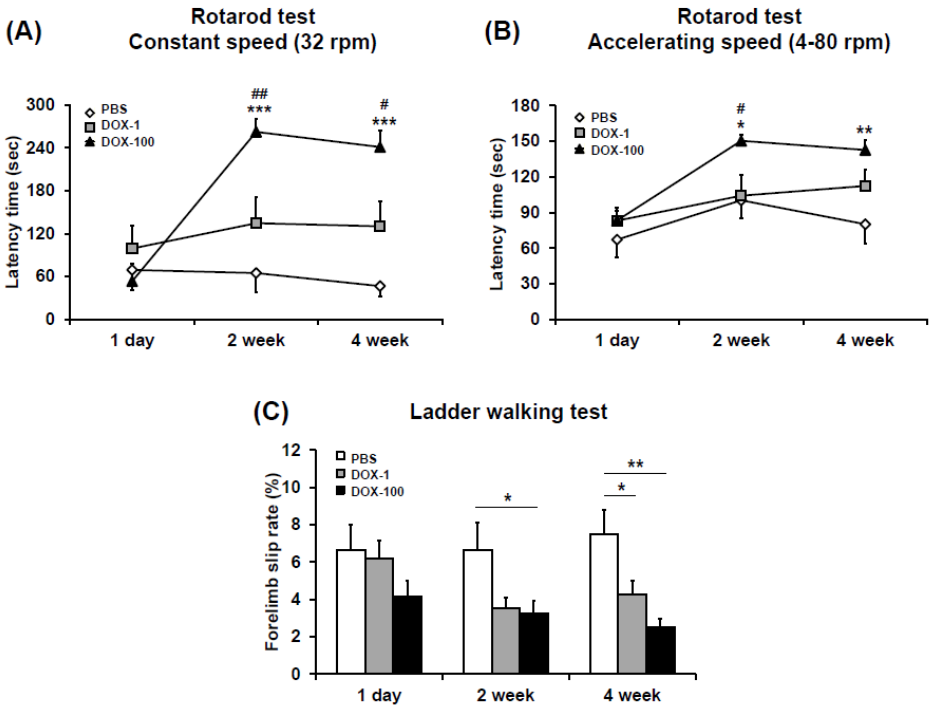

Figure 16. *In vivo* reprogramming factor expression enhanced recovery of neurobehavioral functions in mice with cerebral ischemia. (A, B) Neurobehavioral functions were evaluated by rotarod tests at constant (32 rpm) and accelerating (4-80 rpm) speed and by ladder walking tests (C). Neurobehavioral functions in the DOX-100 group were significantly better than in the phosphate-buffered saline (PBS) controls at 2 and 4 weeks after the ischemic injury (n = 7/group; *P < 0.05; **P < 0.01 and ***P < 0.001 versus PBS, #P < 0.05, ##P < 0.01 versus DOX-1, one-way ANOVA followed by a post-hoc Bonferroni comparison). mean + SEM.

H. Both sham-operated reprogrammable mice and C57BL6/J mice with bilateral common carotid artery occlusion were unaffected by doxycycline

To provide insight into the effects of reprogramming factor expression in mice in the absence of brain ischemia, reprogrammable mice were subjected to a sham operation (in which occlusion of the carotid arteries did not occur) and then were treated with PBS, DOX-1, or DOX-100 via an osmotic pump. Up to 4 weeks post-surgery, the three groups exhibited no differences in rotarod performance (Figure 17A, B). This result suggests that *in vivo* reprogramming factor expression has no beneficial effect on sham-operated reprogrammable mice in the absence of brain ischemia and indicates that the protective effects of the reprogramming factors are ischemia-dependent. In addition, C57BL/6J wild-type mice were subjected to bilateral common carotid artery occlusion and then treated with PBS, DOX-1, or DOX-100. Although doxycycline has been shown to have a neuroprotective effect in a previously published paper,[72] in this study the rotarod performances of these mice did not differ between groups up to 4 weeks after surgery in this study (Figure 17C, D).

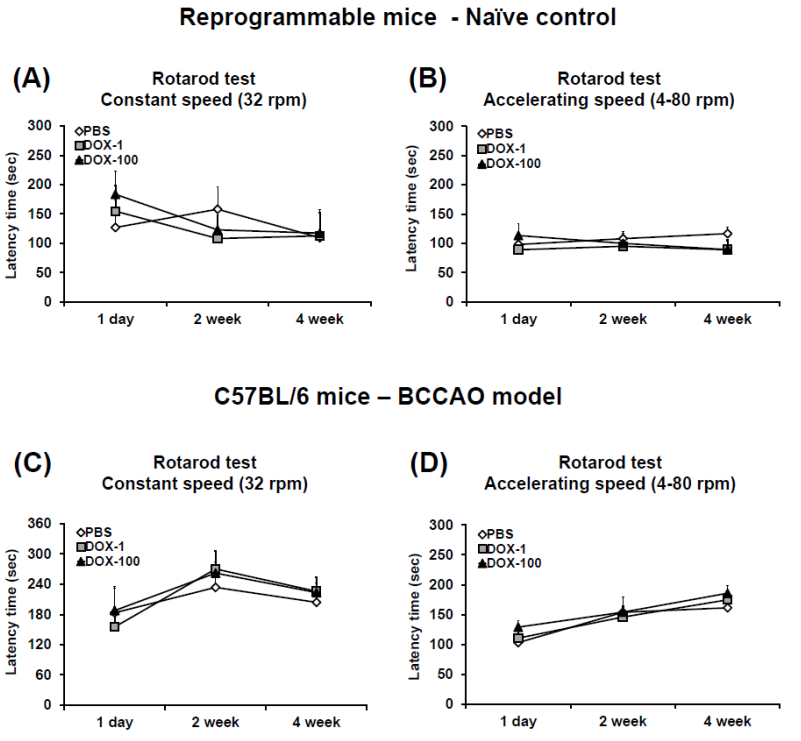

Figure 17. Neurobehavioral evaluation in both sham-operated reprogrammable mice and C57BL6/J mice with bilateral common carotid artery occlusion. The sham-operated reprogrammable mice and C57BL6/J mice with bilateral common carotid artery occlusion were given PBS, DOX-1 or DOX-100 and evaluated by the rotarod test at constant (32 rpm) and accelerating speed (4-80 rpm). (A, B) Up to 4 weeks after surgery, there was no difference among the three groups in rotarod performances of sham-operated reprogrammable mice without occlusion of carotid artery. mean + SEM (n = 6, 6, and 5 for DOX-100, DOX-1, and PBS groups, respectively. (C, D) Similarly, the rotarod performances of C57BL/6J mice with bilateral common carotid artery occlusion and infused with PBS, DOX-1 or DOX-100 via an osmotic pump were not different up to 4 weeks after surgery. mean + SEM (n = 5, 4, and 5 for DOX-100, DOX-1, and PBS groups, respectively).

I. Virus-mediated reprogramming factor expression improved behavioral function in mice with cerebral ischemia

To evaluate reprogramming factor expression in the control mice, the lateral ventricles of C57BL/6J mice were injected with either 4 μl of a viral vector expressing the four reprogramming factors (CytoTuneTM–iPS Sendai Reprogramming Kit, Life Technologies, Carlsbad, CA) or with enhanced green fluorescent protein (EGFP) (CytoTuneTM–EmGFP Sendai Fluorescence Reporter, Life Technologies) following BCCAO (Figure 18A, B). To determine whether this reprogramming factor-induced functional recovery would also occur in the control C57BL/6J mice with transient global brain ischemia induced by 20 minutes of BCCAO, we delivered the four reprogramming factors using viral vector through intraventricular injection. Confocal microscopy showed virus-mediated expression of Oct4 and EGFP in the ventricular zone (Figure 18C), indicating that transgenes were expressed by viral vectors in this region. The rotarod test showed a tendency toward improved latency periods in the reprogramming factor-expressing viral vector group as compared to the GFP-expressing group, although this tendency was statistically significant only in the accelerating speed test administered at 4 weeks post-BCCAO (Figure 18D; $P < 0.05$). Ladder walking tests also revealed that the forelimb slip rate (%) in the reprogramming factor-expressing group was 1.5 times lower than in the GFP-expressing group (Figure 18E; $P < 0.05$). This modest tendency toward improved neurobehavioral function in the control mice as compared with the doxycycline-inducible reprogrammable mice might be, at least in part, due to the limited expression of reprogramming factors by the nature of viral vector and doxycycline.

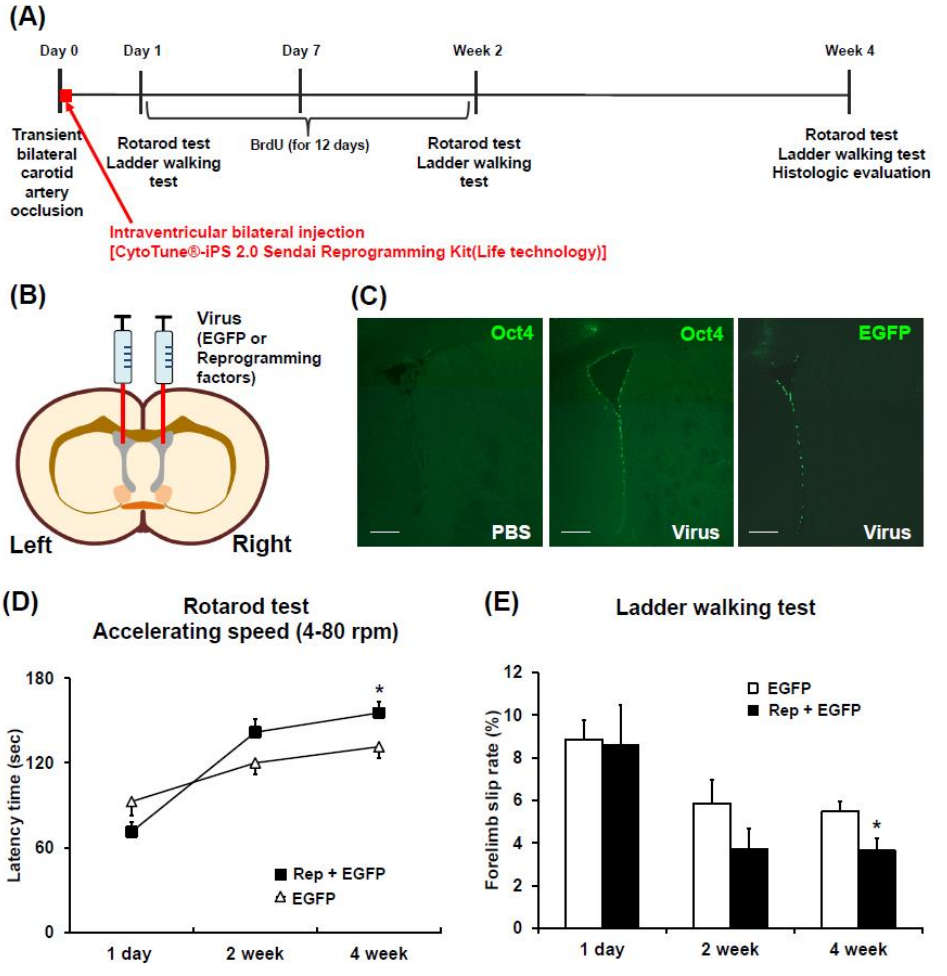

Figure 18. Study design and reprogramming factor delivery via viral vector enhanced functional recovery. (A, B) Study design. Transient global cerebral ischemia was induced by 20-minute bilateral carotid artery occlusion (two vessel occlusion) in the C57BL/6J mice. Thereafter, the reprogramming factor-expressing viral vector or GFP-expressing viral vector (virus control) was infused once into the right and left lateral ventricle using a stereotaxic surgery frame (B) and BrdU was daily injected for 12 days. Behavioral tests such as the rotarod and ladder walking tests were performed. Four weeks after the cerebral ischemia induction, the mice were euthanized and histologically analyzed. (C) Three days

after the injection of PBS or viral vector, the expression of Pou5f1 (Oct4) and EGFP was evaluated using confocal microscopy. (D, E) Neurobehavioral functions were evaluated by rotarod test at constant speed and by ladder walking test. The rotarod test at accelerating speed (4-80 rpm) and forelimb slip rate in ladder walking test showed that neurobehavioral functions in the reprogramming factor-expressing group (n = 9/group) were significantly better than in the EGFP-expressing control group (n = 10/group) at 4 weeks after the ischemic injury (*P < 0.05, Student's t-test). Scale bar = 200 μm.

J. Down-regulated genes were profiled by transcriptome sequencing

To elucidate the mechanism underlying the therapeutic effects outlined above, total RNA was prepared for RNA sequencing from samples obtained from the brains of mice in the PBS and DOX-100 groups (n = 5/group) at 4 weeks after induction of reprogramming factors. The transcriptome analysis was performed using RNA sequencing in order to identify genes differentially expressed among the groups, with a cut-off fold change of 1.5 (P < 0.05). Among down-regulated genes, a total of 9 genes were selected: 3 genes associated with astrocytes (GFAP, Vimentin, and S100β) and 6 genes associated with complements (C3, C4a, C4b, C1qa, C1qb, and C1qc) (Table 3).

Table 3. Differentially expressed genes (DEGs) in down-regulated genes

Downregulated genes at 4 weeks after treatment	
Gene symbol	DOX-100 / PBS
C3	-7.958315
C4a	-1.771182
C4b	-3.5
C1qa	-2.204425
C1qb	-2.249906
C1qc	-2.232664
GFAP	-2.629414
Vimentin	-2.563695
S100β	-1.141646

K. Down-regulated genes were validated using qRT-PCR

A hallmark of several neurological disorders is the presence of activated microglia and harmful astrocytes activated by complements, which impairs synaptogenesis and compromises neuronal survival.[73] The down-regulated genes of interest, complements such as C3, C4a, C4b, C1qa, C1qb, and C1qc, and astrocyte markers such as GFAP, Vimentin, and S100β were validated using qRT-PCR. In particular, the complements family is known to a marker of astrocytes, indicating detrimental functions. These genes were significantly down-regulated in the DOX-treated group compared to the PBS control group, confirming the results of the RNA (Figure 19; $P < 0.05$, $P < 0.01$, $P < 0.001$).

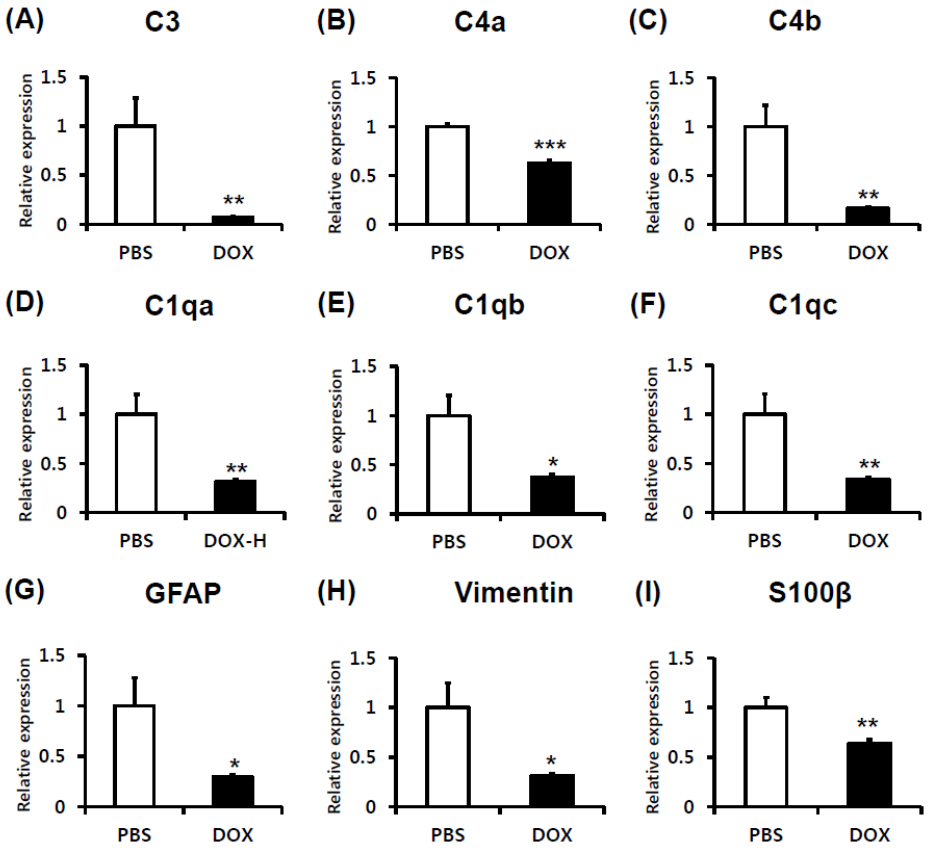

Figure 19. RNA-sequencing results were validated by quantitative real-time qRT-PCR. (A-I) Total RNA was isolated from the brains of mice at 4-week after treatment of doxycycline. The qRT-PCR confirmed that complement C3, C4a, C4b, C1qa, C1qb, C1qc, and astrocyte marker such as GFAP, Vimentin and S100β significantly decreased in DOX-100 treated mice. mean + SEM (n = 4/group; *P < 0.05, **P < 0.01, *** P < 0.001, Student's t-test).

L. *In vivo* reprogramming factor expression decreased C3 expression in astrocytes

In 2017, two review papers about reactive astrocytes showed that A1 astrocytes might have detrimental functions, including the promotion of neurodegeneration, neurotoxicity, and synaptic impairments, whereas A2 astrocytes might have beneficial functions, including the promotion of neuroprotection and neural repair. Many markers have been identified that distinguish reactive astrocytes;[48] in particular, complement C3 is known to be an A1-astrocyte specific marker.[44,74] C3 expression was therefore confirmed in astrocytes, and the results indicated that *in vivo* reprogramming factor expression in doxycycline-treated group appeared to decrease C3 in A1 astrocytes compared to the PBS control group (Figure 20; $P < 0.05$).

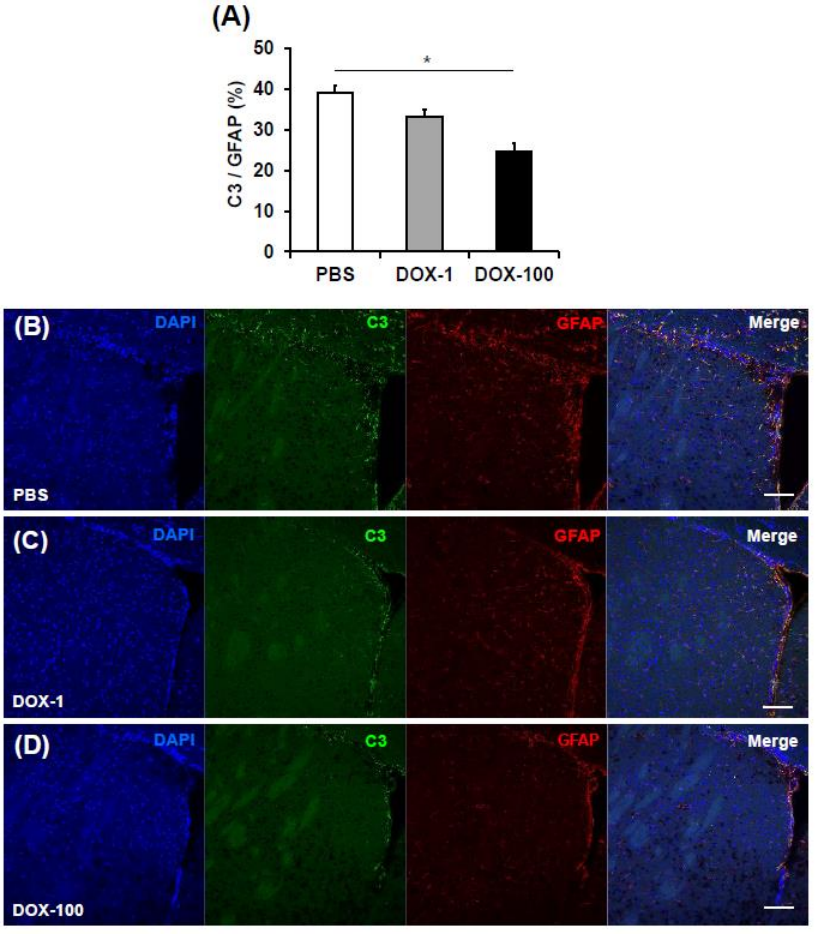

Figure 20. $C3^+$ cells were significantly decreased by transient reprogramming expression in reactive astrocytes. Four weeks after transient ischemic insult, percentage of co-localization of C3 and GFAP were analyzed. (A) *In vivo* transient reprogramming factor expression in doxycycline group dose-dependently decreased C3 expression in A1 astrocytes compared to the PBS control (n = 3/group; *P < 0.05). (B-D) Representative fluorescent microscopic images. Scale bar = 100 μm. mean + SEM

2. Hypoxic-ischemic (HI) brain injury model

Based on the results of previous studies in BCCAO mice, HI mice were used to confirm the dose-dependent effects of *in vivo* expression of reprogramming factors. With the aim of finding a better therapeutic approach by observing differences in effect according to injection region, doxycycline was injected into both the lateral ventricle and the striatum. The experimental design for the HI mouse model is described in Figure 21.

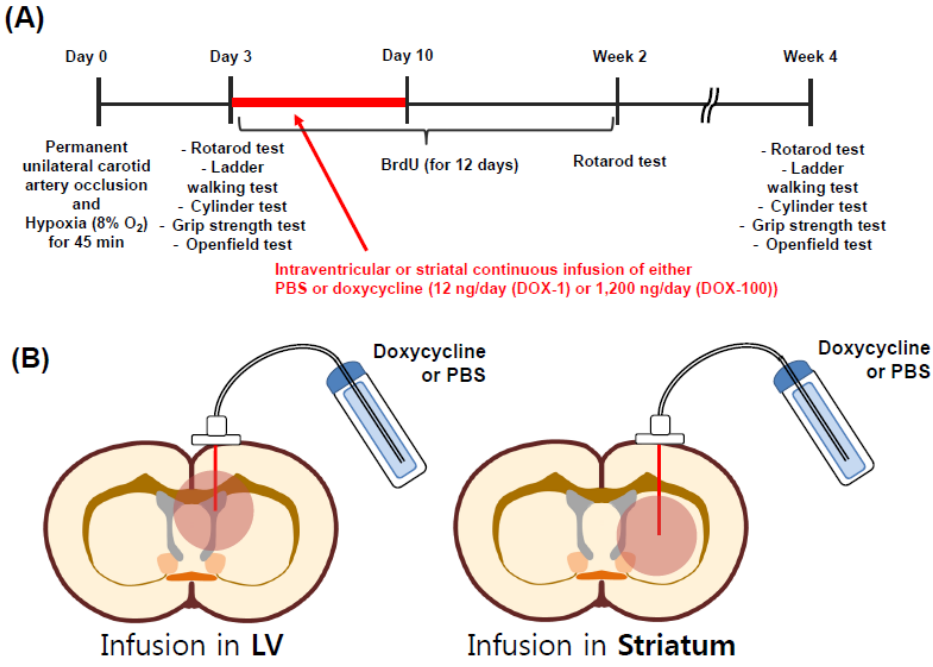

Figure 21. Experimental design and doxycycline injection. (A) Experimental design. Hypoxic-ischemic injury was induced by right carotid artery ligation in the DOX-inducible reprogrammable mice, and hypoxia was induced at 8% O_2 (92% N_2) for 45 minutes. Thereafter, DOX (DOX-1, 1 μg/ml; DOX-100, 100 μg/ml) or PBS was continuously infused into the right lateral ventricle via an osmotic pump over 7 days and BrdU was daily injected for 12 days. Behavioral

tests such as the rotarod test, ladder walking test, cylinder test, grip strength test and openfield test were performed. Four weeks after the cerebral ischemia induction, the mice were euthanized and histologically analyzed. (B) DOX injection into both the lateral ventricle (left side) and the striatum (right side) via an osmotic pump to infuse DOX-1 (12 ng/day) or DOX-100 (1,200 ng/day).

A. *In vivo* reprogramming factor expression facilitated asymmetry improvement after hypoxic-ischemic brain injury, but not in the rotarod motor function test

To determine whether *in vivo* reprogramming factor expression enhances functional recovery in the HI brain damage model, neurobehavioral functions were evaluated using the rotarod test, ladder walking, cylinder, grip strength, and openfield tests.

Rotarod tests at constant (32 rpm) and accelerating (4-80 rpm) speeds indicated no differences in performance among the three groups (PBS, DOX-1, and DOX-100) in both the lateral ventricle-targeted and striatum-targeted groups (Figure 22 A-D), suggesting that reprogramming factor expression did not contribute in motor function recovery in the HI mouse model. Similarly, Pollak et al. observed clear deficits in HI mice compared to sham control mice, but there was no significant difference at 1 month after HI insult.[6]

In the grip strength test, grip power in the contralateral hemiplegic limb of DOX-100 treated mice in the lateral ventricle-targeted group at 4 weeks after doxycycline treatment (65.0 ± 2.7 gram × force) was significantly improved compared to 1 day after doxycycline treatment (54.6 ± 4.7; $P < 0.01$) (Figure 23D), but no difference was observed in the striatum-targeted group (Figure 23A). Therefore, *in vivo* reprogramming factor expression can, under certain circumstances, induce improvement in grip strength.

In the ladder walking test and the cylinder test, which evaluate fine motor coordination and asymmetry, the contralateral forelimb slip rates relative to total

steps in the DOX-100 group at 4 weeks post-treatment were 0.9 ± 0.3%, which is 5.3 times lower than in the DOX-100 group at 1-day post-treatment (4.8 ± 0.7%; $P < 0.001$). The forelimb slip rate in both the DOX-1 and PBS groups were no significance over time. In addition, in the striatum-targeted group, infusion of doxycycline had no therapeutic effect on HI mice. The cylinder test revealed significant improvement in the percentage of cylinder wall contacts with the hemiplegic forelimb only in the DOX-100 group at 4 weeks post-treatment (42.5 ± 6.6%) compared to the same group at 1-day post-treatment (13.9 ± 7.0%; $P < 0.05$) (Figure 23). In addition, there are no differences noted in the striatum-targeted groups. Taken together, the cylinder and ladder walking test results suggest forelimb-use asymmetry can be improved following the inducement of reprogramming factor expression in cases of HI brain injury. Interestingly, the groups, that received a doxycycline injection into the striatum showed no functional recovery in any test evaluating behavioral function. Selecting the correct injection site therefore appears to be important for effective treatment.

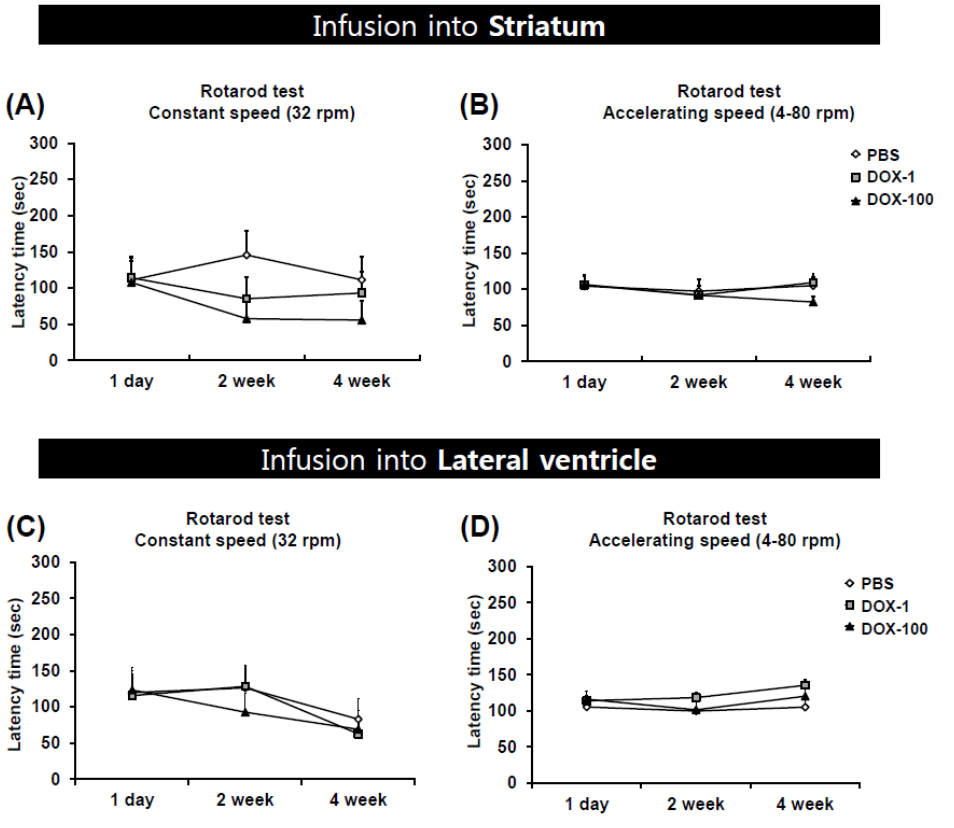

Figure 22. There were no changes by induction of reprogramming factor in mice with HI injury. Functions were evaluated by rotarod tests at constant (32 rpm) and accelerating speed (4-80 rpm). However, both group, DOX-infusion into striatum (A, B) and lateral ventricle (C, D), showed that there was no difference in rotarod performances in among the groups (n = 8 and 9 for striatum-targeted group and lateral ventricle-targeted groups, respectively). mean + SEM.

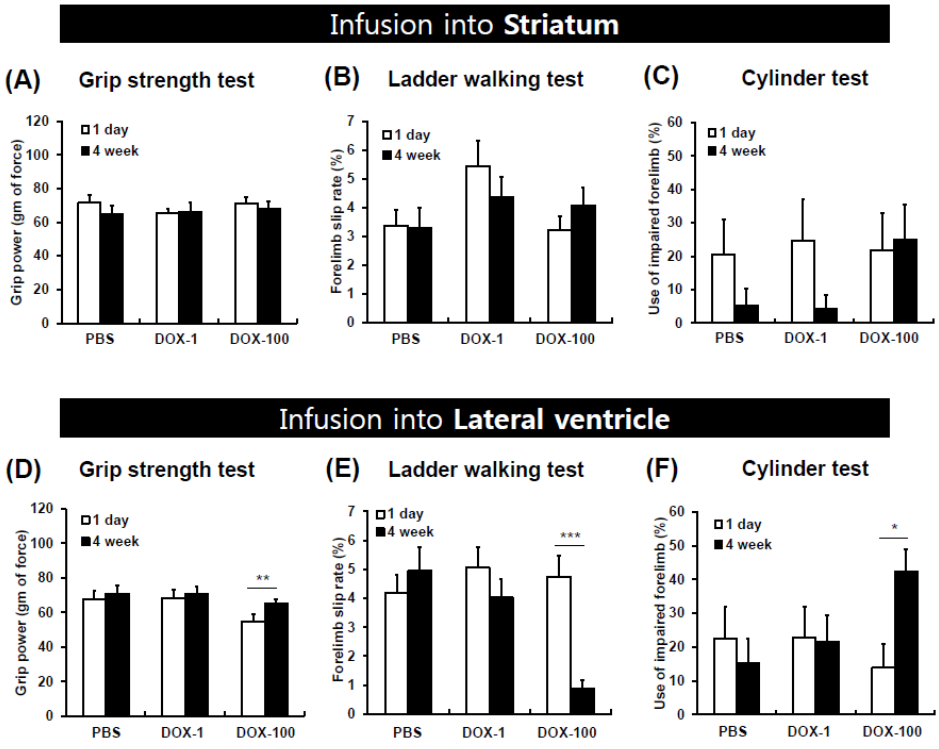

Figure 23. Asymmetry was alleviated in the lateral ventricle-targeted group, but not in the striatum-targeted group. Neurobehavioral hemiplegic functions were evaluated by grip strength test, ladder walking test and cylinder test. (A-C) Function of contralateral hemiplegic limb in striatum-targeted group has no change between 1 day and 4 weeks (n = 8/group). (D) The grip power of hemiplegic limb showed significant enhancements in DOX-100 treated mice at 4 weeks compared to 1 day (n = 9/group; **P < 0.01, student's t-test). (E, F) The percentage of use of impaired forelimb improved in DOX-100 group at 4 weeks compared to 1 day (n = 9/group; **P < 0.01 and ***P < 0.001, student's t-test). mean + SEM.

B. *In vivo* reprogramming factor expression alleviates anxiety-like behavior in the open field test

An open field test was administered to examine not only locomotor activity but also tendency to prefer staying in specific areas, such as in the corners, on the side, or in the center zone.[75] The striatum-targeted groups showed nonsignificant changes in distance from the corner zones between 1 day and 4 weeks following DOX–treatment. However, distance from the corner zones significantly decreased in DOX-100 mice in the lateral ventricle-targeted groups at 4 weeks post-treatment ($P < 0.05$ versus 1 day), suggesting that reprogramming factor expression alleviated anxiety-like behavior in HI injured mice (Figure 24).

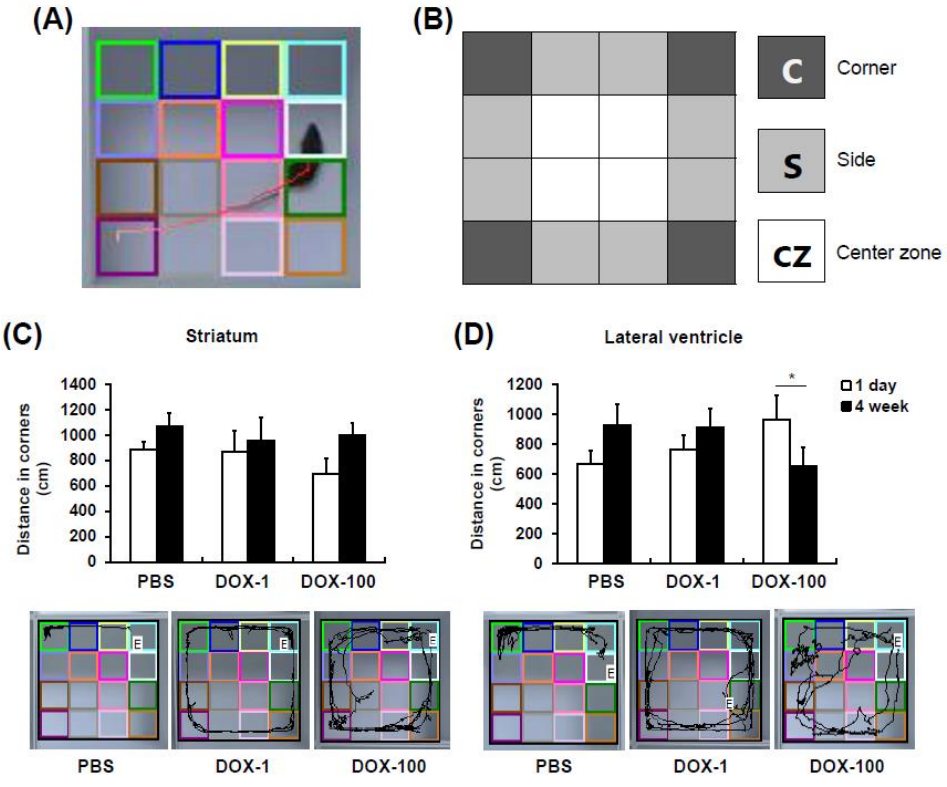

Figure 24. Anxiety-like behavior was attenuated in DOX-100 treated mice of the lateral ventricle-targeted group, but not in the striatum-targeted group. Open field tests were performed at 1 day and 4 weeks after DOX-treatment. (A) Representative image of open field test. (B) A square box illustrates a schematic test area of open field test and shows areas designated as the corners, sides, and center zones. (C, D) Distance in corners were not changed by reprogramming expression in striatum-targeted groups (n = 8/groups). But, lateral ventricle-targeted group showed that distance in corners decreased at 4 weeks after induction of reprogramming factors (n = 9/group; *P < 0.01, student's t-test). mean + SEM.

C. Tumor formation following 1,000 μg/ml doxycycline injection into the striatum

To confirm the existence of brain tumor formation, injections of doxycycline (1, 100, and 1,000 μg/ml) and PBS were performed in both lateral ventricle and striatum. The results showed that tumor development was observed in the group that received an infusion of doxycycline into the striatum (Figure 25). Likewise, proper dose of expression of reprogramming factor should be carefully considered when targeting the injection site (either the lateral ventricle or striatum).

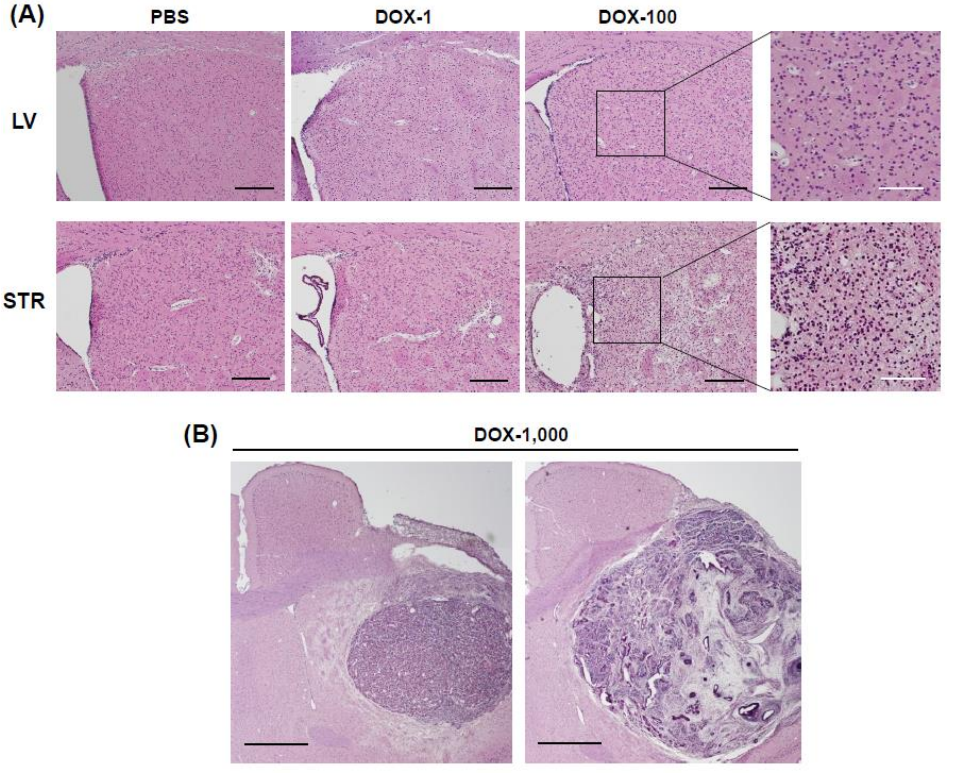

Figure 25. Tumor-like tissue formation was not observed in DOX-1 and DOX-100 but it showed tumor-like tissues in DOX-1,000. (A) When

reprogramming factor is introduced into the lateral ventricle region, tumor was not observed. However, in the striatum infusion group, when treated with doxycycline 100 μg/ml, tissue in abnormal condition were observed. (B) Injecting DOX-1,000 in striatum showed tumor formation. Scale bar = 200 μm.

D. *In vivo* reprogramming factor expression increased new astrocytes in the subventricular zone and striatum

To express the reprogramming factors in the damaged brain tissues of *in vivo* HI mice, an osmotic pump was used to infuse either doxycycline or control buffer (PBS) into the lateral ventricle, as described above.

Histological result showed that the number of $BrdU^+$ cells in the subventricular zone in mice in the DOX-100 groups was 3.8 times higher than in the PBS control group ($P < 0.05$), while the number of $BrdU^+$ cells in the DOX-100 group was 1.7 times higher than in the DOX-1 group. The number of $BrdU^+GFAP^+$ cells in the DOX-100 group was 3.6 times higher than in the PBS control group ($P < 0.01$), suggesting that reprogramming factor expression causes a robust proliferative generation of astrocytes (Figure 26). Likewise, in the BCCAO model, the number of $BrdU^+$βIII-tubulin$^+$ cells were similar across all groups, suggesting that neurogenesis in the subventricular zone is not affected by the reprogramming factors.

Next, the density of astrocytes was evaluated in order to confirm the presence of cell generation through proliferation in the striatum. The density of $BrdU^+GFAP^+$ cells in region 1 in the DOX-100 group was significantly higher than in the DOX-1 and PBS groups ($P < 0.01$) (Figure 27). Taken together, these data indicate that the densities of all proliferated cells and proliferated astrocytes were significantly higher in the striatum regions closer to the lateral ventricle.

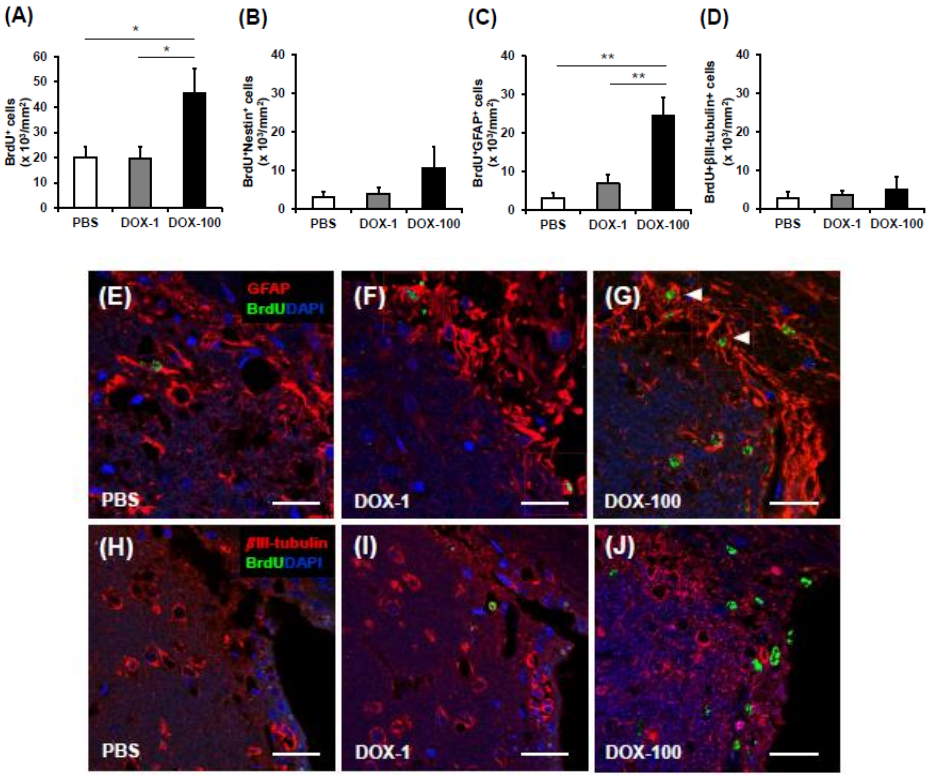

Figure 26. Increased number of newly generated cells and astrocytes induced by reprogramming factor expression in the subventricular zone. After the induction of focal ischemia, the DOX-inducible reprogrammable mice were infused with two doses of doxycycline (12 ng/day, DOX-1; 1,200 ng/day, DOX-100) or PBS into the right lateral ventricle for 7 days. To identify newly generated cells, the mice were daily injected daily with 5-bromo-2-deoxyuridine (BrdU) for 12 days. Four weeks after ischemia induction, histologic evaluations were performed. The density of newly generated neural progenitors, astrocytes, and neurons was determined through confocal microscopy by calculating the density of cells triple positive for DAPI (blue, nuclei), BrdU (green), and cell type-specific markers such as Nestin, GFAP, and βIII-tubulin, respectively. (A, C) The density of $BrdU^+$ cells and $BrdU^+GFAP^+$ cells in the subventricular zone were

significantly higher in both the DOX-100 than in the other groups (n = 3-4/group; *P < 0.05, **P < 0.01 one-way ANOVA followed by a post-hoc Bonferroni comparison). (B, D) The densities of $BrdU^+Nestin^+$ and $BrdU^+\beta III\text{-tubulin}^+$ cells in both the DOX-100 and DOX-1 groups were presented no significance among the groups. (n = 3-4/group). (E-J) Representative confocal microscopic images. Scale bars = 25 μm. mean + SEM.

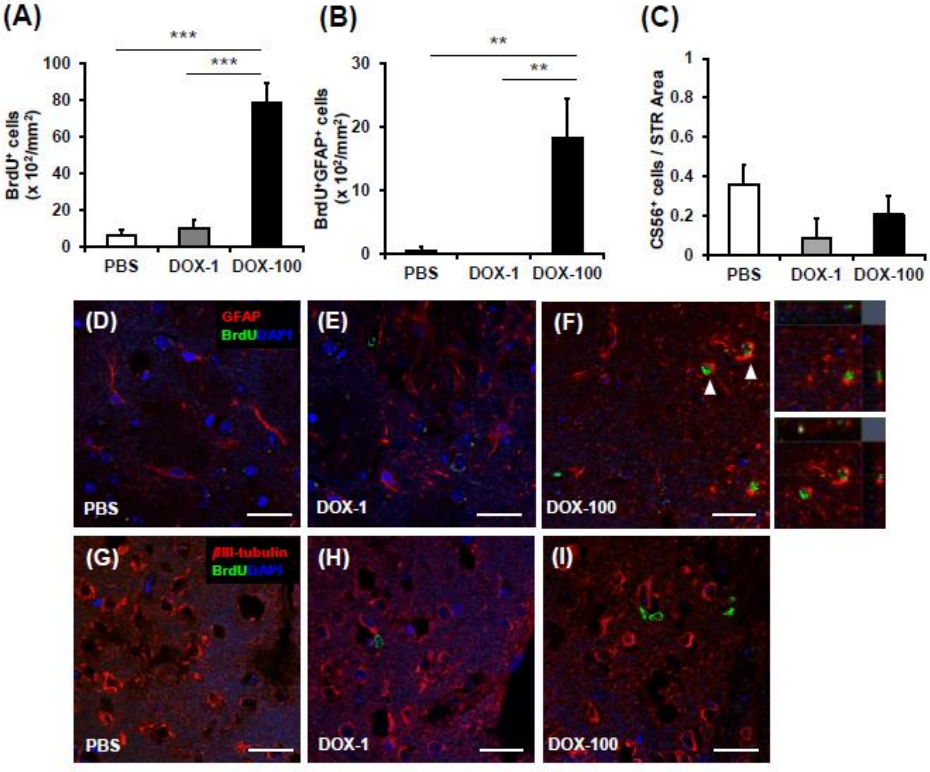

Figure 27. Reprogramming factor expression increased the number of newly generated astrocytes in the striatum. (A) The densities of $BrdU^+$ cells in the striatum of DOX-100 group were significantly higher than in both DOX-1 group and PBS controls (n = 3-4/group; ***P < 0.001, one-way ANOVA followed by a post-hoc Bonferroni comparison). The density of newly generated astrocytes

and neurons was determined through confocal microscopy by calculating the density of cells triple positive for DAPI (blue, nuclei), BrdU (green), and cell type-specific markers such as GFAP and βIII-tubulin, respectively. (B) The density of $BrdU^+GFAP^+$ cells, but not $BrdU^+$βIII-$tubulin^+$ cells, was significantly higher in the DOX-100 group than in the DOX-1 and PBS groups (n = 3-4/group; **P < 0.01, one-way ANOVA followed by a post-hoc Bonferroni comparison). (C) The density of area positive for CS-56, a marker of glial scar. The area of CS-56 staining did not differ among the groups (n = 3-4/group). (D-I) Representative confocal microscopic images of $BrdU^+GFAP^+$ cells and $BrdU^+$βIII-$tubulin^+$ cells in the striatum. Scale bars = 25 μm. mean + SEM. CS-56, chondroitin sulfate-56.

E. *In vivo* reprogramming factor expression enhanced angiogenesis and neuroprotection

Evaluation of blood vessel density in the striatum via tissue staining indicated that the number of $CD31^+$ capillaries in the DOX-100 group was 1.6 and 1.9 times higher than in the PBS control and DOX-1 groups, respectively (P < 0.05) (Figure 28). To confirm the neuroprotective effect, the density of NeuN+ cells in the striatum was determined using qRT-PCR and immunohistochemistry. As a result, expression of striatal NeuN increased significantly in mice treated with DOX-100 compared to mice in the DOX-1 and PBS groups (P < 0.01) (Figure 29). Therefore, *in vivo* reprogramming factor expression contributed to neuroprotection and angiogenesis following HI injury conditions.

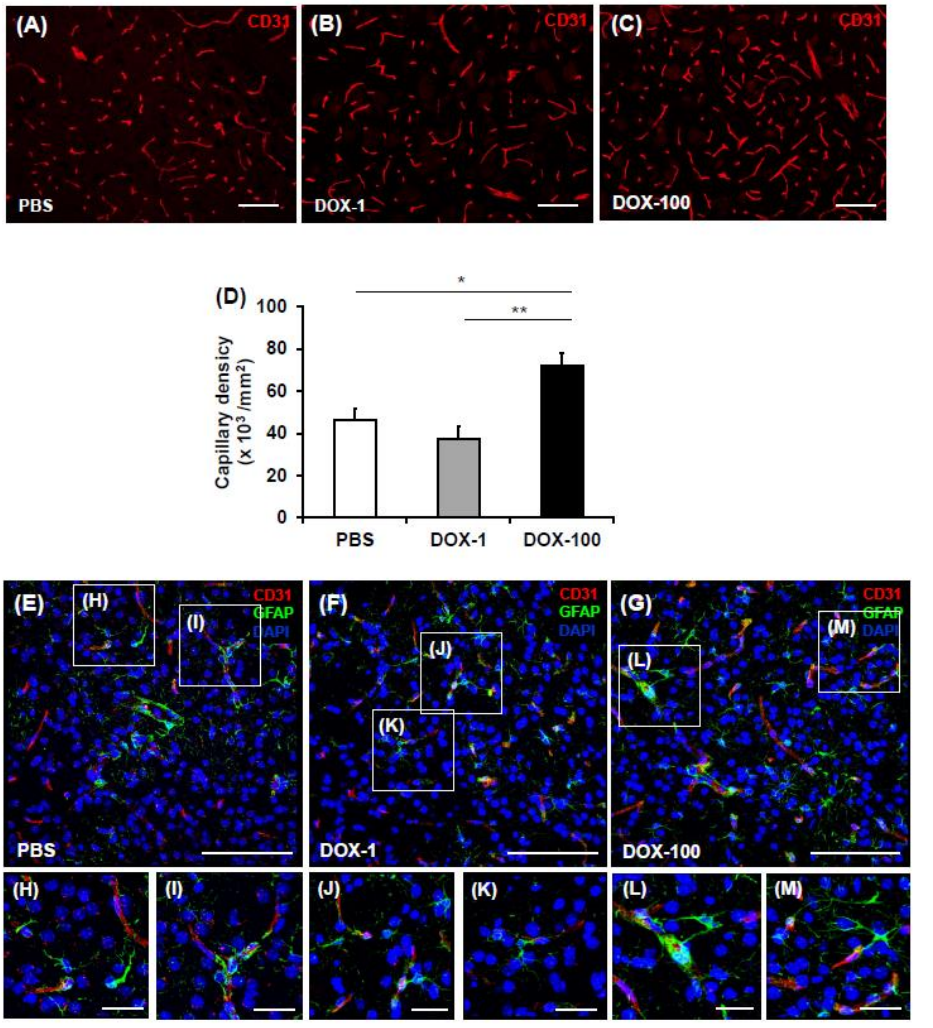

Figure 28. Angiogenesis was enhanced by reprogramming factor expression in the striatum. Four weeks after ischemia induction, the blood vessel density was determined by immunofluorescent staining against CD31. (A-C) Representative fluorescent microscopic images. Scale bar = 100 μm. (D) The density of $CD31^+$ capillaries in the striatum was significantly higher in DOX-100 group than in both the DOX-1 and PBS controls. (n = 5/group; *P < 0.05 and **P < 0.01 respectively, one-way ANOVA followed by a post-hoc Bonferroni

comparison). (E-M) Confocal microscopic pictures showing blood vessels close to astrocytes. $CD31^+$ endothelial cells lining blood vessels are surrounded with $GFAP^+$ astrocytes in PBS, DOX-1, and DOX-100 groups. Scale bar = 25 μm. mean + SEM. CD31, cluster of differentiation 31.

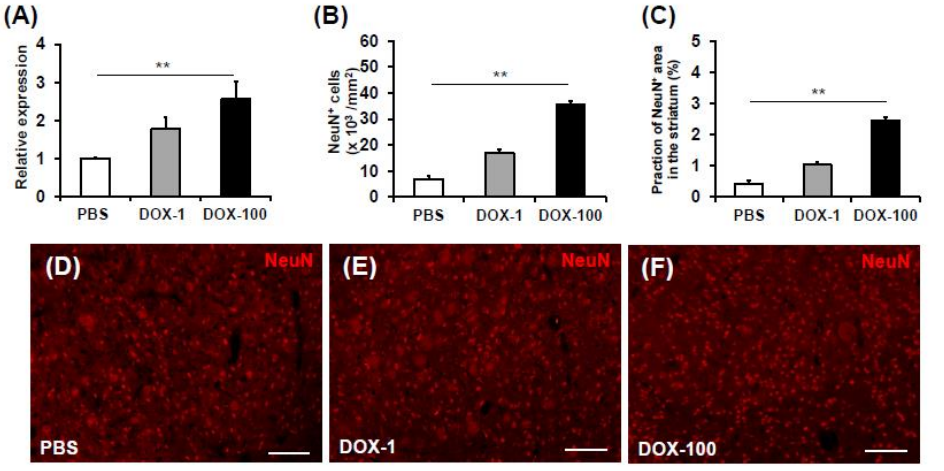

Figure 29. *In vivo* reprogramming factor expression enhanced neural survival. (A) Gene expression of markers of neural survival was evaluated by qRT-PCR. Expression of striatal NeuN significantly increased in mice treated with DOX-100 compared to the PBS control group (n = 4-5/group; **P < 0.01, one-way ANOVA followed by a post-hoc Bonferroni comparison) (B, C) The number of $NeuN^+$ cells (/mm^3) and the fraction of area that was NeuN+ in the striatum (%) were significantly higher in mice treated with DOX-100 than PBS control group (n = 4-5/group; **P < 0.01, one-way ANOVA followed by a post-hoc Bonferroni comparison). (D-F) Representative fluorescent microscopic images of $NeuN^+$ cells in the striatum. Scale bar = 100 μm. mean + SEM.

IV. DISCUSSION

Although *in vivo* expression of reprogramming factors has been studied with respect to tumor development[63] and reprogramming into pluripotency,[64] whether these factors can augment functional restoration in brains that have suffered ischemic injury has not yet been investigated.

1. Functional recovery and proliferation neural cells (neural progenitors and astrocytes) in brain injury

In this study, reprogramming factor-induced functional recovery was associated with proliferative generation of $Nestin^+$ or $GFAP^+$ cells in the subventricular zone and striatum. Given that the early responses to reprogramming factor expression include cell proliferation,[9,76] the source of these cells could be endogenous $Nestin^+$ cells (neural progenitors) and $GFAP^+$ cells (astrocytes), respectively. However, it cannot be ruled out that these cells could be also derived from other cell types because transient overexpression of reprogramming factors can epigenetically activate the cells into an intermediate plastic state that allows cells to take on alternate fates.[9,20-22,77,78] Elucidating the source of these newly generated neural progenitors and astrocytes would require complex lineage tracing experiments,[9,79,80] which are beyond the scope of the current study. Because functional improvement was associated with selective expansion of neural progenitors and astrocytes, it might be speculated that these cell types are required for recovery from brain injury and the prevention of additional tissue damage. This idea is in line with previous results showing that neural stem/progenitor cells, but not mature neurons, can lead to functional recovery when transplanted into damaged brain tissue[81,82] and that astrocytes are responsible for the prevention of tissue damage and neuronal loss in several mouse models of brain injury.[9,47] Our data are also compatible with results from a previous interesting report showing that gliogenic, but not neurogenic, neural

stem/progenitor cells promoted axonal growth, remyelination, angiogenesis, and locomotor functional recovery when transplanted into a mouse model of spinal cord injury.[9,83]

2. Responses of astrocytes to brain injury

Here in the brain ischemia models, reprogramming factor-induced astrogliosis was associated with functional restoration and angiogenesis, which is compatible with previous studies showing that astrogliosis has beneficial effects in the acute phase of injury.[9,47,84] However, the long-term consequence of astrogliosis could be detrimental.[9,47,84] It can produce glial scar formation and prevent neurogenesis from endogenous progenitors or transplanted stem/progenitor cells, as well as axonal regeneration. In this study, gliogenesis induced by *in vivo* reprogramming factor expression did not increase the glial scar formation in the striatum of the damaged brains. Thus, the $GFAP^+$ cells generated by reprogramming factor expression might be a novel cell source with stem cell potential in the injured brain.[9,84]

Reactive astrocytes are divided into two subtypes, A1 astrocytes and A2 astrocytes, which are induced by neuroinflammation and ischemia, respectively.[37] Many papers have demonstrated that A1 astrocytes might have detrimental functions, while A2 astrocytes might have beneficial functions.[37,44] A1 astrocytes, in particular, are known to create negative interactions via NFkB signaling in neurodegenerative diseases such as Alzheimer's disease, Parkinson's disease, and Huntington's disease.[44,85-88] The complement C3, one of the A1 astrocyte markers, has been shown to exacerbate infarct volume in cerebral ischemia with hypoxia.[52] Therefore, it will help the recovery process in ischemic brain injury by *in vivo* reprogramming factors-induced astrocytes via the decreased expression of C3.

3. Angiogenesis and astrocytes

Angiogenesis is essential for recovery from ischemic injury. The role of

astrocytes in angiogenesis in the retina, a part of the central nervous system like the brain, has been relatively well characterized;[9,89,90] here, astrocytes form a template that guides retinal angiogenesis in both normal development and injury-associated regeneration. Although the role of astrocytes in brain angiogenesis has yet to be elucidated, astrocytes have been proposed to be the cell type that forms the trophic microenvironment that supports angiogenesis and enables the survival of transplanted striatal tissue in the human brain.[9,91] In this study, key angiogenic factors robustly expressed in astrocytes might contribute to this trophic environment that favors angiogenesis and tissue regeneration. Furthermore, it is well established that astrocytes contribute to the formation of the blood-brain barrier, which is compatible with our results showing that $CD31^+$ blood vessels are surrounded by $GFAP^+$ cells. Previous studies have shown that astrocytes, which produce the proangiogenic and neurogenic factors such as FGF2 and VEGFA, can facilitate angiogenesis and neurogenesis and enhance functional recovery after cerebral ischemia and hypoxic-ischemic brain injury.[9,92-94] Taken together, these results suggest that reprogramming factor-induced functional recovery might be mediated by the proliferative generation of astrocytes, which express factors that are both angiogenic and neurogenic.

4. Synaptic plasticity and astrocytes

Astrocytes are the main neural-lineage cell type for the maintenance of brain homeostasis and contribute to neuroprotection and neuron survival via the secretion of neurotransmitters, cytokines and growth factors.[9,70,71] In this study, *in vivo* expression of reprogramming factors induced an increase in the number of newly generated astrocytes without effects on neurogenesis, providing further evidence of motor function recovery. Expression of NeuN (a mature neuronal marker), synaptophysin (a presynaptic marker), and PSD95 (a postsynaptic marker) also increased in a doxycycline-dependent manner, suggesting increased neuronal survival and synaptic plasticity. These results might provide an

explanation for the relationship between newly generated astrocytes induced by *in vivo* reprogramming factor expression and functional recovery. Additional experiments revealed that sham-operated reprogrammable mice (that is, reprogrammable mice that lacked occlusion of the carotid artery) that received either PBS, DOX-1, or DOX-100 showed no beneficial effect in the absence of brain ischemia in the rotarod test up to 4 weeks after surgery, suggesting that the protective effects of reprogramming factors are ischemia-dependent.

5. Induction of reprogramming factor and tumor formation

It has recently been reported that doxycycline-induced *in vivo* expression of reprogramming factors can lead to the development of teratoma.[64] Similar tumors have previously been observed in mice in which Pou5f1 (Oct4) expression was induced by doxycycline *in vivo*.[9,63] However, tumor development was not observed in this study. This discrepancy may be attributable to differences between our study and the others in terms of both delivery methods and the tissues analyzed. In each of the other studies, doxycycline was systemically administered to the mice through drinking water,[9,63,64] whereas in our study doxycycline was injected into the lateral ventricle in our study, where the systemic effects of doxycycline would be minimal or negligible. Among the three existing studies, one study,[9,64] but not the other two, showed the expression of reprogramming factors in brain tissue. However, tumor development in the brain was not observed in this study. In all three studies, tumor development was observed predominantly in epithelial tissues in the stomach, intestine, pancreas, kidney, and skin, but not in the brain.

V. CONCLUSION

In conclusion, this study has shown that *in vivo* transient expression of the four reprogramming factors promoted functional recovery in mouse models of cerebral ischemia. This facilitated functional recovery was associated with enhanced angiogenesis together with the proliferative generation of astrocytes and/or neural progenitors. *In vivo* reprogramming factor-mediated functional restoration provides insight into the mechanisms underlying recovery from tissue damage and potentially enables the development of novel therapeutic modalities to facilitate recovery from tissue injury such as cerebral ischemia.

REFERENCES

1. Hartman RE, Lee JM, Zipfel GJ, Wozniak DF. Characterizing learning deficits and hippocampal neuron loss following transient global cerebral ischemia in rats. Brain Res 2005;1043:48-56.
2. Smith ML, Bendek G, Dahlgren N, Rosen I, Wieloch T, Siesjo BK. Models for studying long-term recovery following forebrain ischemia in the rat. 2. A 2-vessel occlusion model. Acta Neurol Scand 1984;69:385-401.
3. Pulsinelli WA, Brierley JB, Plum F. Temporal profile of neuronal damage in a model of transient forebrain ischemia. Ann Neurol 1982;11:491-8.
4. Kirino T, Tsujita Y, Tamura A. Induced tolerance to ischemia in gerbil hippocampal neurons. J Cereb Blood Flow Metab 1991;11:299-307.
5. Ravichandran Ranjithkumar PP, Muthiah Ramanathan. Measurement of inflammatory mediators at different time intervals after neuronal injury induced by bilateral common carotid artery occlusion model. Journal of pharmaceutical sciences and research 2015;7:662-7.
6. Pollak J, Doyle KP, Mamer L, Shamloo M, Buckwalter MS. Stratification substantially reduces behavioral variability in the hypoxic-ischemic stroke model. Brain Behav 2012;2:698-706.
7. Levine S. Anoxic-ischemic encephalopathy in rats. Am J Pathol 1960;36:1-17.
8. Adhami F, Liao G, Morozov YM, Schloemer A, Schmithorst VJ, Lorenz JN, et al. Cerebral ischemia-hypoxia induces intravascular coagulation and autophagy. Am J Pathol 2006;169:566-83.
9. Seo JH, Lee MY, Yu JH, Kim MS, Song M, Seo CH, et al. In Situ Pluripotency Factor Expression Promotes Functional Recovery From Cerebral Ischemia. Mol Ther 2016;24:1538-49.
10. Iihoshi S, Honmou O, Houkin K, Hashi K, Kocsis JD. A therapeutic window for intravenous administration of autologous bone marrow after cerebral ischemia in adult rats. Brain Res 2004;1007:1-9.
11. Chen J, Li Y, Wang L, Lu M, Zhang X, Chopp M. Therapeutic benefit of intracerebral transplantation of bone marrow stromal cells after cerebral ischemia in rats. J Neurol Sci 2001;189:49-57.
12. Park KI, Teng YD, Snyder EY. The injured brain interacts reciprocally with neural stem cells supported by scaffolds to reconstitute lost tissue. Nat Biotechnol 2002;20:1111-7.
13. Delcroix GJ, Schiller PC, Benoit JP, Montero-Menei CN. Adult cell therapy for brain neuronal damages and the role of tissue engineering. Biomaterials 2010;31:2105-20.

14. Roitberg B. Transplantation for stroke. Neurol Res 2004;26:256-64.
15. Fong SP, Tsang KS, Chan AB, Lu G, Poon WS, Li K, et al. Trophism of neural progenitor cells to embryonic stem cells: neural induction and transplantation in a mouse ischemic stroke model. J Neurosci Res 2007;85:1851-62.
16. Im SH, Yu JH, Park ES, Lee JE, Kim HO, Park KI, et al. Induction of striatal neurogenesis enhances functional recovery in an adult animal model of neonatal hypoxic-ischemic brain injury. Neuroscience 2010;169:259-68.
17. Cho SR, Benraiss A, Chmielnicki E, Samdani A, Economides A, Goldman SA. Induction of neostriatal neurogenesis slows disease progression in a transgenic murine model of Huntington disease. J Clin Invest 2007;117:2889-902.
18. Benraiss A, Toner MJ, Xu Q, Bruel-Jungerman E, Rogers EH, Wang F, et al. Sustained mobilization of endogenous neural progenitors delays disease progression in a transgenic model of Huntington's disease. Cell Stem Cell 2013;12:787-99.
19. Takahashi K, Yamanaka S. Induction of pluripotent stem cells from mouse embryonic and adult fibroblast cultures by defined factors. Cell 2006;126:663-76.
20. Efe JA, Hilcove S, Kim J, Zhou H, Ouyang K, Wang G, et al. Conversion of mouse fibroblasts into cardiomyocytes using a direct reprogramming strategy. Nat Cell Biol 2011;13:215-22.
21. Kurian L, Sancho-Martinez I, Nivet E, Aguirre A, Moon K, Pendaries C, et al. Conversion of human fibroblasts to angioblast-like progenitor cells. Nat Methods 2013;10:77-83.
22. Zhu S, Rezvani M, Harbell J, Mattis AN, Wolfe AR, Benet LZ, et al. Mouse liver repopulation with hepatocytes generated from human fibroblasts. Nature 2014;508:93-7.
23. Maza I, Caspi I, Zviran A, Chomsky E, Rais Y, Viukov S, et al. Transient acquisition of pluripotency during somatic cell transdifferentiation with iPSC reprogramming factors. Nat Biotechnol 2015;33:769-74.
24. Vierbuchen T, Ostermeier A, Pang ZP, Kokubu Y, Sudhof TC, Wernig M. Direct conversion of fibroblasts to functional neurons by defined factors. Nature 2010;463:1035-41.
25. Lujan E, Chanda S, Ahlenius H, Sudhof TC, Wernig M. Direct conversion of mouse fibroblasts to self-renewing, tripotent neural precursor cells. Proc Natl Acad Sci U S A 2012;109:2527-32.
26. Vierbuchen T, Wernig M. Direct lineage conversions: unnatural but useful? Nat Biotechnol 2011;29:892-907.
27. Meyer K, Ferraiuolo L, Miranda CJ, Likhite S, McElroy S, Renusch S, et al. Direct conversion of patient fibroblasts demonstrates non-cell

autonomous toxicity of astrocytes to motor neurons in familial and sporadic ALS. Proc Natl Acad Sci U S A 2014;111:829-32.
28. Chanda S, Marro S, Wernig M, Sudhof TC. Neurons generated by direct conversion of fibroblasts reproduce synaptic phenotype caused by autism-associated neuroligin-3 mutation. Proc Natl Acad Sci U S A 2013;110:16622-7.
29. Guo Z, Zhang L, Wu Z, Chen Y, Wang F, Chen G. In vivo direct reprogramming of reactive glial cells into functional neurons after brain injury and in an Alzheimer's disease model. Cell Stem Cell 2014;14:188-202.
30. Niu W, Zang T, Zou Y, Fang S, Smith DK, Bachoo R, et al. In vivo reprogramming of astrocytes to neuroblasts in the adult brain. Nat Cell Biol 2013;15:1164-75.
31. Torper O, Pfisterer U, Wolf DA, Pereira M, Lau S, Jakobsson J, et al. Generation of induced neurons via direct conversion in vivo. Proc Natl Acad Sci U S A 2013;110:7038-43.
32. Smith ZD, Nachman I, Regev A, Meissner A. Dynamic single-cell imaging of direct reprogramming reveals an early specifying event. Nat Biotechnol 2010;28:521-6.
33. Mikkelsen TS, Hanna J, Zhang X, Ku M, Wernig M, Schorderet P, et al. Dissecting direct reprogramming through integrative genomic analysis. Nature 2008;454:49-55.
34. Baudino TA, McKay C, Pendeville-Samain H, Nilsson JA, Maclean KH, White EL, et al. c-Myc is essential for vasculogenesis and angiogenesis during development and tumor progression. Genes Dev 2002;16:2530-43.
35. Hirayama Y, Koizumi S. Astrocytes and ischemic tolerance. Neurosci Res 2018;126:53-9.
36. Choudhury GR, Ding S. Reactive astrocytes and therapeutic potential in focal ischemic stroke. Neurobiol Dis 2016;85:234-44.
37. Liddelow SA, Guttenplan KA, Clarke LE, Bennett FC, Bohlen CJ, Schirmer L, et al. Neurotoxic reactive astrocytes are induced by activated microglia. Nature 2017;541:481-7.
38. Sofroniew MV, Vinters HV. Astrocytes: biology and pathology. Acta Neuropathol 2010;119:7-35.
39. Clarke LE, Barres BA. Emerging roles of astrocytes in neural circuit development. Nat Rev Neurosci 2013;14:311-21.
40. Chung WS, Clarke LE, Wang GX, Stafford BK, Sher A, Chakraborty C, et al. Astrocytes mediate synapse elimination through MEGF10 and MERTK pathways. Nature 2013;504:394-400.
41. Liddelow S, Barres B. SnapShot: Astrocytes in Health and Disease. Cell 2015;162:1170- e1.

42. Anderson MA, Burda JE, Ren Y, Ao Y, O'Shea TM, Kawaguchi R, et al. Astrocyte scar formation aids central nervous system axon regeneration. Nature 2016;532:195-200.
43. Sofroniew MV. Astrogliosis. Cold Spring Harb Perspect Biol 2014;7:a020420.
44. Liddelow SA, Barres BA. Reactive Astrocytes: Production, Function, and Therapeutic Potential. Immunity 2017;46:957-67.
45. Lian H, Yang L, Cole A, Sun L, Chiang AC, Fowler SW, et al. NFkappaB-activated astroglial release of complement C3 compromises neuronal morphology and function associated with Alzheimer's disease. Neuron 2015;85:101-15.
46. Colombo E, Farina C. Astrocytes: Key Regulators of Neuroinflammation. Trends Immunol 2016;37:608-20.
47. Sofroniew MV. Molecular dissection of reactive astrogliosis and glial scar formation. Trends Neurosci 2009;32:638-47.
48. Zamanian JL, Xu L, Foo LC, Nouri N, Zhou L, Giffard RG, et al. Genomic analysis of reactive astrogliosis. J Neurosci 2012;32:6391-410.
49. Stevens B, Allen NJ, Vazquez LE, Howell GR, Christopherson KS, Nouri N, et al. The classical complement cascade mediates CNS synapse elimination. Cell 2007;131:1164-78.
50. Christopherson KS, Ullian EM, Stokes CC, Mullowney CE, Hell JW, Agah A, et al. Thrombospondins are astrocyte-secreted proteins that promote CNS synaptogenesis. Cell 2005;120:421-33.
51. Eroglu C, Allen NJ, Susman MW, O'Rourke NA, Park CY, Ozkan E, et al. Gabapentin receptor alpha2delta-1 is a neuronal thrombospondin receptor responsible for excitatory CNS synaptogenesis. Cell 2009;139:380-92.
52. Ten VS, Sosunov SA, Mazer SP, Stark RI, Caspersen C, Sughrue ME, et al. C1q-deficiency is neuroprotective against hypoxic-ischemic brain injury in neonatal mice. Stroke 2005;36:2244-50.
53. Colombo E, Cordiglieri C, Melli G, Newcombe J, Krumbholz M, Parada LF, et al. Stimulation of the neurotrophin receptor TrkB on astrocytes drives nitric oxide production and neurodegeneration. J Exp Med 2012;209:521-35.
54. Chen A, Xiong LJ, Tong Y, Mao M. The neuroprotective roles of BDNF in hypoxic ischemic brain injury. Biomed Rep 2013;1:167-76.
55. Akaike A, Katsuki H, Kume T, Maeda T. Reactive oxygen species in NMDA receptor-mediated glutamate neurotoxicity. Parkinsonism Relat Disord 1999;5:203-7.
56. Chen Y, Swanson RA. Astrocytes and brain injury. J Cereb Blood Flow Metab 2003;23:137-49.

57. Carey BW, Markoulaki S, Beard C, Hanna J, Jaenisch R. Single-gene transgenic mouse strains for reprogramming adult somatic cells. Nat Methods 2010;7:56-9.
58. Wu C, Zhan RZ, Qi S, Fujihara H, Taga K, Shimoji K. A forebrain ischemic preconditioning model established in C57Black/Crj6 mice. J Neurosci Methods 2001;107:101-6.
59. Lee SW, Kim WJ, Choi YK, Song HS, Son MJ, Gelman IH, et al. SSeCKS regulates angiogenesis and tight junction formation in blood-brain barrier. Nat Med 2003;9:900-6.
60. Cho SR, Kim YR, Kang HS, Yim SH, Park CI, Min YH, et al. Functional recovery after the transplantation of neurally differentiated mesenchymal stem cells derived from bone marrow in a rat model of spinal cord injury. Cell Transplant 2009;18:1359-68.
61. Won YH, Lee MY, Choi YC, Ha Y, Kim H, Kim DY, et al. Elucidation of Relevant Neuroinflammation Mechanisms Using Gene Expression Profiling in Patients with Amyotrophic Lateral Sclerosis. PLoS One 2016;11:e0165290.
62. Kim MS, Yu JH, Lee MY, Kim AL, Jo MH, Kim M, et al. Differential Expression of Extracellular Matrix and Adhesion Molecules in Fetal-Origin Amniotic Epithelial Cells of Preeclamptic Pregnancy. PLoS One 2016;11:e0156038.
63. Hochedlinger K, Yamada Y, Beard C, Jaenisch R. Ectopic expression of Oct-4 blocks progenitor-cell differentiation and causes dysplasia in epithelial tissues. Cell 2005;121:465-77.
64. Abad M, Mosteiro L, Pantoja C, Canamero M, Rayon T, Ors I, et al. Reprogramming in vivo produces teratomas and iPS cells with totipotency features. Nature 2013;502:340-5.
65. Morshead CM, Reynolds BA, Craig CG, McBurney MW, Staines WA, Morassutti D, et al. Neural stem cells in the adult mammalian forebrain: a relatively quiescent subpopulation of subependymal cells. Neuron 1994;13:1071-82.
66. Alvarez-Buylla A, Garcia-Verdugo JM. Neurogenesis in adult subventricular zone. J Neurosci 2002;22:629-34.
67. Pencea V, Bingaman KD, Wiegand SJ, Luskin MB. Infusion of brain-derived neurotrophic factor into the lateral ventricle of the adult rat leads to new neurons in the parenchyma of the striatum, septum, thalamus, and hypothalamus. J Neurosci 2001;21:6706-17.
68. Arai K, Jin G, Navaratna D, Lo EH. Brain angiogenesis in developmental and pathological processes: neurovascular injury and angiogenic recovery after stroke. FEBS J 2009;276:4644-52.
69. Lee HS, Han J, Bai HJ, Kim KW. Brain angiogenesis in developmental and pathological processes: regulation, molecular and cellular

communication at the neurovascular interface. FEBS J 2009;276:4622-35.
70. Belanger M, Magistretti PJ. The role of astroglia in neuroprotection. Dialogues Clin Neurosci 2009;11:281-95.
71. Takuma K, Baba A, Matsuda T. Astrocyte apoptosis: implications for neuroprotection. Prog Neurobiol 2004;72:111-27.
72. Wang Z, Xue Y, Jiao H, Liu Y, Wang P. Doxycycline-mediated protective effect against focal cerebral ischemia-reperfusion injury through the modulation of tight junctions and PKCdelta signaling in rats. J Mol Neurosci 2012;47:89-100.
73. Hajishengallis G, Reis ES, Mastellos DC, Ricklin D, Lambris JD. Novel mechanisms and functions of complement. Nat Immunol 2017;18:1288-98.
74. Baldwin KT, Eroglu C. Molecular mechanisms of astrocyte-induced synaptogenesis. Curr Opin Neurobiol 2017;45:113-20.
75. Hattiangady B, Mishra V, Kodali M, Shuai B, Rao X, Shetty AK. Object location and object recognition memory impairments, motivation deficits and depression in a model of Gulf War illness. Front Behav Neurosci 2014;8:78.
76. Plath K, Lowry WE. Progress in understanding reprogramming to the induced pluripotent state. Nat Rev Genet 2011;12:253-65.
77. Ladewig J, Koch P, Brustle O. Leveling Waddington: the emergence of direct programming and the loss of cell fate hierarchies. Nat Rev Mol Cell Biol 2013;14:225-36.
78. Kim J, Ambasudhan R, Ding S. Direct lineage reprogramming to neural cells. Curr Opin Neurobiol 2012;22:778-84.
79. Hsieh PC, Segers VF, Davis ME, MacGillivray C, Gannon J, Molkentin JD, et al. Evidence from a genetic fate-mapping study that stem cells refresh adult mammalian cardiomyocytes after injury. Nat Med 2007;13:970-4.
80. Senyo SE, Steinhauser ML, Pizzimenti CL, Yang VK, Cai L, Wang M, et al. Mammalian heart renewal by pre-existing cardiomyocytes. Nature 2013;493:433-6.
81. Rhee YH, Ko JY, Chang MY, Yi SH, Kim D, Kim CH, et al. Protein-based human iPS cells efficiently generate functional dopamine neurons and can treat a rat model of Parkinson disease. J Clin Invest 2011;121:2326-35.
82. Kim SU, de Vellis J. Stem cell-based cell therapy in neurological diseases: a review. J Neurosci Res 2009;87:2183-200.
83. Kumagai G, Okada Y, Yamane J, Nagoshi N, Kitamura K, Mukaino M, et al. Roles of ES cell-derived gliogenic neural stem/progenitor cells in functional recovery after spinal cord injury. PLoS One 2009;4:e7706.

84. Robel S, Berninger B, Gotz M. The stem cell potential of glia: lessons from reactive gliosis. Nat Rev Neurosci 2011;12:88-104.
85. Kaltschmidt B, Uherek M, Volk B, Baeuerle PA, Kaltschmidt C. Transcription factor NF-kappaB is activated in primary neurons by amyloid beta peptides and in neurons surrounding early plaques from patients with Alzheimer disease. Proc Natl Acad Sci U S A 1997;94:2642-7.
86. Mori T, Koyama N, Arendash GW, Horikoshi-Sakuraba Y, Tan J, Town T. Overexpression of human S100B exacerbates cerebral amyloidosis and gliosis in the Tg2576 mouse model of Alzheimer's disease. Glia 2010;58:300-14.
87. Hunot S, Brugg B, Ricard D, Michel PP, Muriel MP, Ruberg M, et al. Nuclear translocation of NF-kappaB is increased in dopaminergic neurons of patients with parkinson disease. Proc Natl Acad Sci U S A 1997;94:7531-6.
88. Hsiao HY, Chen YC, Chen HM, Tu PH, Chern Y. A critical role of astrocyte-mediated nuclear factor-kappaB-dependent inflammation in Huntington's disease. Hum Mol Genet 2013;22:1826-42.
89. Alkayed NJ, Harukuni I, Kimes AS, London ED, Traystman RJ, Hurn PD. Gender-linked brain injury in experimental stroke. Stroke 1998;29:159-65; discussion 66.
90. Gibson CL. Cerebral ischemic stroke: is gender important? J Cereb Blood Flow Metab 2013;33:1355-61.
91. Cisbani G, Freeman TB, Soulet D, Saint-Pierre M, Gagnon D, Parent M, et al. Striatal allografts in patients with Huntington's disease: impact of diminished astrocytes and vascularization on graft viability. Brain 2013;136:433-43.
92. Briones TL, Woods J, Wadowska M, Rogozinska M, Nguyen M. Astrocytic changes in the hippocampus and functional recovery after cerebral ischemia are facilitated by rehabilitation training. Behav Brain Res 2006;171:17-25.
93. Seo JH, Kim H, Park ES, Lee JE, Kim DW, Kim HO, et al. Environmental enrichment synergistically improves functional recovery by transplanted adipose stem cells in chronic hypoxic-ischemic brain injury. Cell Transplant 2013;22:1553-68.
94. Krum JM, Mani N, Rosenstein JM. Roles of the endogenous VEGF receptors flt-1 and flk-1 in astroglial and vascular remodeling after brain injury. Exp Neurol 2008;212:108-17.

ABSTRACT (IN KOREA)

뇌허혈 마우스 모델에서 재프로그래밍 인자의 생체내 발현을 통한 성상교세포의 치료 가능성

<지도교수 조 성 래>

연세대학교 대학원 의과학과

서 정 화

뇌허혈과 뇌졸중은 치료 불가능한 손상을 유도 또는 사망으로 이르게 한다. 뇌에서 가장 풍부한 세포 중 하나인 성상교세포는 허혈과 같은 손상된 조건에서 활성화된다. 이러한 반응성 성상교세포는 뇌손상 회복에 중요한 역할을 한다. 네 가지 리프로그래밍 인자(Pou5f1, Sox2, Myc, Klf4)의 일시적인 발현은 세포 유형을 전환시키는데 사용되었지만 허혈성 손상으로부터 기능회복을 촉진하는 수단으로는 거의 연구되지 않았다. 본 연구에서 생체내 일시적 리프로그래밍 발현이 신경 행동 기능을 향상시킬 수 있는지 확인하고자 한다.

뇌허혈은 일시적 양측 총경동맥 폐쇄 (BCCAO)와 저산소증(8% O_2)을 동반하는 영구적인 단일 총경동맥 결찰(HI)의 두가지 방법에 의해 유도되며, 그 후 네 가지 리프로그래밍 인자가 독시사이클린에 의해 발현되는 유전자변이 마우스의 뇌 (뇌실 또는 선조체)에 독시사이클을 처치한다. 독시사이클린(DOX-1; 1μg/ml, DOX-100; 100μg/ml) 또는 인산염 완충 식염수(PBS)를 삼투압펌프를 이용하여 연속적으로 7일간 주입하였다.

BCCAO 모델에서 조직 학적 평가 결과, 이 일시적인 리프로그래밍 인자 발현은 신경 세포가 아닌 성상교세포 및 신경전구세포의 증식을 유도하고 혈관 신생 인자의 상승 조절을 통해 신생 혈관 형성을 증가시키는 것을 확인하였다. 또한, 생체내 리프로그래밍인자 발현은 선조체에서 성숙한 뉴런의 수 및 시냅스 형성의 증가와 같은 신경 보호 효과를 유도 하였다. 게다가 리프로그래밍 유도에 의한 종양 발달은 관찰되지 않았다. 중요한 것은 rotarod 및 사다리 보행 테스트와 같은 신경 행동 평가 결과 생체내 일시적 리프로그래밍 발현이 허혈성 손상으로부터 기능 회복을 촉진한다는 것을 확인하였다. 성상교세포 증식과 관련된 치료기전 규명을 위해 DOX-100 그룹과 PBS 그룹에 비해 DOX-100 그룹에서 유의미하게 변화된 전사체(transcriptome)을 찾기 위해 RNA sequencing analysis를 시행하였다. 보체 C3, C4a, C4b, C1qa, C1qb, C1qc 그리고 성상교세포 마커들과 같은 감소된 유전자들을 qRT-PCR 을 이용하여 검증하였다. 특히 C3 는 유해한 성상교세포 마커이기 때문에 C3를 조직학적 분석을 통해 정량화하였다. 그 결과 C3는 생체내 리프로그래밍 인자 발현에 의해 유의미하게 감소하였다.

다른 실험 그룹으로 사용되는 뇌졸중 모델인 허혈성 저산소성 손상 모델을 사용하였는데, 이 실험에서는 효능이 검증된 리프로그래밍 발현을 뇌의 두 부위, 뇌실과 선조체에서 실행하여 주입 부위에 따른 효과를 비교하고자 하였다. 결과적으로, 생체내 리프로그래밍 인자 발현 후 손상된 뇌에서 성상교세포와 신경전구세포는 유의미하게 증식되었지만, 뉴런이나 신경교상흔은 증식하지 않았으며, 혈관이 강화되었다. 게다가 생체내 다능성인자 발현은 저산소성 허혈성 상태에서 신경세포의 보호를 야기하였다. 그립강도, 실린더, 사다리 워킹 테스트 및 오픈필드 테스트와 같은 신경행동 평가는 네가지 리프로그래밍 인자의 뇌실에서의 발현을 통해 기능회복을 극적으로 촉진한다는 것을 보여주었다. 흥미롭게, 선조체에서 리프로그래밍 발현은 그룹간의 신경학적기능의 변화를 가져오지 않았다. rotarod 테스트에서는 뇌실 및 선조체 표적 군 모두에서 유의미한 차이가 없었다. 뇌실 표적 군에서 종양 발달은 관찰되지 않았지만, 선조체 표적 군에서 DOX-100 처리 마우스에서 비정상 상태를 보였다. 또한, 선조체 표적 군에서 DOX-100(doxycycline; 1,000 μg/ml)의 처치는 종양을 형성하였다. 선조체에서 리프로그래밍 인자를 발현한 마우스의

경우 치료효과를 확인할 수 없었다. 뇌실에서 리프로그래밍 인자를 발현한 그룹에서의 신경조직학적 결과는 신경 세포가 아닌 성상교세포의 증식 및 선조체의 혈관을 증가시키는 것을 확인하였다.

종합하면, 새로 생성된 성상교세포는 대뇌 허혈 (BCCAO 및 HI 마우스 모델)에서 신경세포 보호 및 신혈관 강화에 필수적인 세포이다. 이러한 결과는 BCCAO 마우스 모델 에서 반응성 성상교세포(유해 A1 성상교세포)의 감소를 통한 기능 회복에 대한 치료적 가능성이 있다. HI 마우스 모델에서는 리프로그래밍 인자의 선조체 표적 발현에 회복 효과가 없지만 뇌실 표적 군에서는 그렇지 않다. 따라서 리프로그래밍 인자의 발현을 위해 뇌실을 표적으로 하는 것이 치료를 위한 더 나은 치료법이 될 것이다.

핵심되는 말: 리프로그래밍 인자, 뇌허혈, 기능회복, 반응성 상교세포, 신경보호

PUBLICATION LIST

1. Cho SR, Suh H, Yu JH, Kim HH, **Seo JH**, Seo CH. Astroglial Activation by an Enriched Environment after Transplantation of Mesenchymal Stem Cells Enhances Angiogenesis after Hypoxic-Ischemic Brain Injury. Int J Mol Sci 2016;17.
2. Kim MS, Yu JH, Kim CH, Choi JY, **Seo JH**, Lee MY, et al. Environmental enrichment enhances synaptic plasticity by internalization of striatal dopamine transporters. J Cereb Blood Flow Metab 2016;36:2122-33.
3. **Seo JH**, Lee MY, Yu JH, Kim MS, Song M, Seo CH, et al. *In Situ* Pluripotency Factor Expression Promotes Functional Recovery From Cerebral Ischemia. Mol Ther 2016;24:1538-49.
4. Won YH, Lee MY, Choi YC, Ha Y, Kim H, Kim DY, et al. Elucidation of Relevant Neuroinflammation Mechanisms Using Gene Expression Profiling in Patients with Amyotrophic Lateral Sclerosis. PLoS One 2016;11:e0165290.
5. Yu JH, Kim M, **Seo JH**, Cho S-R. Brain Plasticity and Neurorestoration by Environmental Enrichment. Brain&Neurorehabilitation 2016;9.
6. Yu JH, **Seo JH**, Lee JY, Lee MY, Cho SR. Induction of Neurorestoration From Endogenous Stem Cells. Cell Transplant 2016;25:863-82.
7. Kim M, Yu JH, **Seo JH**, Shin YK, Wi S, Baek A, et al. Neurobehavioral Assessments in a Mouse Model of Neonatal Hypoxic-ischemic Brain Injury. J Vis Exp 2017; doi:10.3791/55838.
8. **Seo JH**, Pyo S, Shin YK, Nam BG, Kang JW, Kim KP, et al. The Effect of Environmental Enrichment on Glutathion-Mediated Xenobiotic Metabolism and Antioxidation in Normal Adult Mice. Front Neurol; Accepted 22 May 2018.